Journal of Physiology (1992), **455**, *pp.* 111–142
With 12 figures
Printed in Great Britain

CALCIUM HOMEOSTASIS IN THE OUTER SEGMENTS OF RETINAL RODS FROM THE TIGER SALAMANDER

BY LEON LAGNADO*, LUIGI CERVETTO† AND PETER A. MCNAUGHTON‡

From the Physiological Laboratory, Downing Street, Cambridge CB2 3EG and the ‡Physiology Group, King's College London, Strand, London WC2R 2LS

(*Received 19 March 1991*)

SUMMARY

1. The processes regulating intracellular calcium in the outer segments of salamander rods have been investigated. The main preparation used was the isolated rod loaded with the Ca^{2+}-sensitive photoprotein aequorin, from which outer segment membrane current and free $[Ca^{2+}]_i$ could be recorded simultaneously. Two other preparations were also used: outer segment membrane current was recorded from intact, isolated rods using a suction pipette, and from detached outer segments using a whole-cell pipette.

2. Measurements of free intracellular $[Ca^{2+}]$ in Ringer solution were obtained from two aequorin-loaded rods. Mean $[Ca^{2+}]_i$ in darkness was 0·41 μM, and after a bright flash $[Ca^{2+}]_i$ fell to below detectable levels ($< 0{\cdot}3$ μM). No release of intracellular Ca^{2+} by a bright flash of light could be detected ($< 0{\cdot}2$ μM).

3. Application of the phosphodiesterase inhibitor 3-isobutyl-1-methylxanthine (IBMX) caused an increase in the size of the light-sensitive current and a rise in $[Ca^{2+}]_i$, but application of IBMX either when the light-sensitive channels had been closed by a bright light or in the absence of external Ca^{2+} caused no detectable rise in $[Ca^{2+}]_i$. It is concluded that IBMX increases $[Ca^{2+}]_i$ by opening light-sensitive channels, and does not release Ca^{2+} from stores within the outer segment.

4. Removal of external Na^+ caused a rise in $[Ca^{2+}]_i$ to around 2 μM and completely suppressed the light-sensitive current.

5. The Na^+–Ca^{2+}, K^+ exchange current in aequorin-loaded rods was activated in first-order manner by internal free calcium, with a mean Michaelis constant, K_{Ca}, of 1·6 μM.

6. The K_{Ca} of the Na^+–Ca^{2+}, K^+ exchange was increased by elevating internal $[Na^+]$.

7. The Michaelis relation between $[Ca^{2+}]_i$ and the activity of the Na^+–Ca^{2+}, K^+ exchange was used to calculate the change in $[Ca^{2+}]_i$ occurring during the response to a bright light. In aequorin-loaded rods in Ringer solution the mean change in free

* Present address: Department of Neurobiology, Sherman Fairchild Science Building, Stanford, CA 94305-5401, USA.

† Present address: Istituto di Neurofisiologia del CNR, Via San Zeno 51, 56100 Pisa, Italy.

MS 9245

$[Ca^{2+}]_i$ after a bright flash was 0·34 μM. In these rods 10% of the dark current was carried by Ca^{2+}.

8. Most of the calcium entering the outer segment was taken up rapidly and reversibly by buffer systems. The time constant of equilibration between free and rapidly bound Ca^{2+} was less than 20 ms. No slow component of calcium uptake was detected.

9. Two components of calcium buffering could be distinguished in the outer segments of aequorin-loaded rods. A buffer of low capacity and high affinity (Michaelis constant $K_{buff} \approx 0{\cdot}7$ μM) was important at free $[Ca^{2+}]_i$ below 1 μM. At high free $[Ca^{2+}]_i$ calcium buffering was dominated by a low-affinity buffer of large capacity.

10. The average ratio of free-to-bound Ca^{2+} at low $[Ca^{2+}]_i$ was 1:74, that is to say one Ca^{2+} ion remains free out of every seventy-five entering the outer segment. At high $[Ca^{2+}]_i$ the ratio fell to 1:16.

11. High- and low-affinity components of internal Ca^{2+} buffering were also observed in intact rods, but the mean capacity of the high-affinity buffer, 241 μM, was an order of magnitude larger than in aequorin-loaded rods. The difference is attributed to loss of this component of the buffer during the process of internal perfusion used to load aequorin.

12. In detached outer segments internally perfused by a whole-cell pipette the capacity of the high-affinity calcium buffer declined with a time constant of around 15 min. It is concluded that this component of buffering is associated with a large, diffusible molecule.

13. During internal perfusion the affinity for Ca^{2+} of the Na^+–Ca^{2+}, K^+ exchange declined relative to that of the high-affinity buffer, probably because the affinity of the Na^+–Ca^{2+}, K^+ exchange is controlled by a diffusible cytoplasmic modulator.

INTRODUCTION

Calcium ions play an important role in the process by which retinal photoreceptors transduce light into an electrical signal. Experiments designed to cause an increase in the free $[Ca^{2+}]$ within the outer segment of rods have shown that Ca^{2+} inhibits the light-sensitive current and slows the time course of the light response (Brown, Coles & Pinto, 1977; Hodgkin, McNaughton, Nunn & Yau, 1984; Hodgkin, McNaughton & Nunn, 1985). The fall in free $[Ca^{2+}]_i$ following the light response (McNaughton, Cervetto & Nunn, 1986; Ratto, Payne, Owen & Tsien, 1988) is involved in the adaptation of photoreceptors to light (Cervetto, Torre, Rispoli & Marroni, 1985; Matthews, Murphy, Fain & Lamb, 1988; Nakatani & Yau, 1988*b*) and this effect is thought to be mediated, at least in part, by an inhibitory action of Ca^{2+} on the guanylate cyclase responsible for synthesizing cGMP, the internal transmitter that opens the light-sensitive channel (Lolley & Racz, 1982; Hodgkin *et al.* 1985; Koch & Stryer, 1988). There is also some evidence to support the idea that calcium acts in a 'push–pull' manner on the concentration of cGMP by prolonging the activity of the phosphodiesterase which hydrolyses cGMP to GMP (Kawamura & Murakami, 1991).

To characterize the role of calcium in photoreception we need information on the level of $[Ca^{2+}]_i$ in darkness and in light and on the pathways for entry, exit and intracellular buffering of calcium. Calcium ions enter the outer segment through the

light-sensitive channels (Hodgkin *et al.* 1985) and are extruded by a Na^+–Ca^{2+}, K^+ exchange (Cervetto, Lagnado, Perry, Robinson & McNaughton, 1989; reviewed by McNaughton, 1990). Within the outer segment the majority of calcium is buffered by a rapid and reversible mechanism (McNaughton *et al.* 1986). In the present paper we report measurements of the free $[Ca^{2+}]_i$ from rods loaded with aequorin and we investigate two main aspects of the control of free Ca^{2+} in rod outer segments: the activation of the Na^+–Ca^{2+}, K^+ exchange transport by free intracellular Ca^{2+}, and the properties of the intracellular mechanisms responsible for the rapid buffering of Ca^{2+}.

We find that in normal external saline the free $[Ca^{2+}]_i$ within the outer segment in darkness is about 0·41 μM and that a bright light causes a decrease in $[Ca^{2+}]_i$. Contrary to other reports (Schröder & Fain, 1984; Fain & Schröder, 1985, 1987, 1990) we find no evidence for a light- or cGMP-dependent release of Ca^{2+} from intracellular stores. The Na^+–Ca^{2+}, K^+ exchange is activated by intracellular Ca^{2+} in a first order manner with a mean K_{Ca} of 1·6 μM. Finally, we confirm by direct measurement the existence of two separate buffer systems, and we characterize their calcium binding properties. Some of these results have been presented to the Physiological Society (Cervetto, Lagnado & McNaughton, 1987, 1988).

METHODS

Rods isolated from the tiger salamander retina (Hodgkin, McNaughton & Nunn, 1987) were used in the present study. In the majority of experiments aequorin was incorporated, using a whole-cell pipette, in order to measure intracellular calcium (McNaughton *et al.* 1986). Outer segment membrane current was simultaneously recorded using the suction pipette method (Baylor, Lamb & Yau, 1979). Intact rods (i.e. rods into which aequorin had not been incorporated) were used in some experiments (see Table 3). To examine the effects of internal perfusion on calcium buffering, isolated outer segments were voltage clamped using the whole-cell method (Lagnado, Cervetto & McNaughton, 1988).

Incorporation of aequorin

Whole-cell pipettes were fabricated on a BB-CH two-stage puller (Mecanex, Geneva) from washed borosilicate glass (1·8 mm diameter; Blaubrand 100 μl micropipettes). Suitable pipettes had an internal diameter of about 0·7 μm.

Aequorin was purchased from Dr J. Blinks (Mayo Medical School, Rochester, MN) as a lyophilized powder. Stock solution with an aequorin concentration of 20 mg ml^{-1} was prepared by adding 50 μl of deionized water containing 5 mM-EDTA to the lyophilized powder. Before an experiment, 0·2 μl of the stock was drawn into a short length of dialysis tubing (Bio Rad; diameter 100 μm, mol. wt cut-off 10000), and was dialysed at 4 °C for a minimum of 30 min against the pipette filling solution (see below).

The system for injecting aequorin into the tip of a whole-cell pipette consisted of a fine polythene tube (800 μm external diameter) which had been drawn down to a diameter of 20 μm at the tip, connected to a 5 μl Hamilton syringe filled with paraffin oil. The injection tube was charged with aequorin by drawing in a short column of air (0·1 μl) followed by 0·1 μl of dialysed aequorin solution, and the tip was positioned within the whole-cell electrode as close as possible to the end (*ca* 100 μm distant).

A suitable isolated rod was drawn inner segment first into the suction electrode and a whole-cell recording made from the outer segment. The aequorin solution was then discharged from the injection tube into the pipette tip. An estimate of the rate of exchange of the pipette contents with the rod outer segment cytoplasm was obtained in some experiments by dialysing the aequorin against a solution containing 33·5 mM $[Na^+]$. On injecting the solution containing raised $[Na^+]$ the light-sensitive current declined with a mean half-time of 35 s (three experiments; results not shown). Since the diffusion coefficient of aequorin is at least 40 times less than that of Na^+ (Baker, Hodgkin & Ridgway, 1971) half-equilibration of aequorin should take at least 20 min. In practice it is not always possible to maintain a good whole-cell recording for this long, and the rod outer

segment was normally loaded for about 10 min. At the end of the loading period the whole-cell pipette was gently withdrawn, leaving the aequorin-loaded rod in the suction pipette.

Behaviour of cells before and after loading with aequorin

Control experiments were carried out to assess whether the process by which aequorin was introduced into the cell had any effects on the light response. Bright flashes were delivered before and after incorporation of aequorin and the time courses of the responses were found to be almost

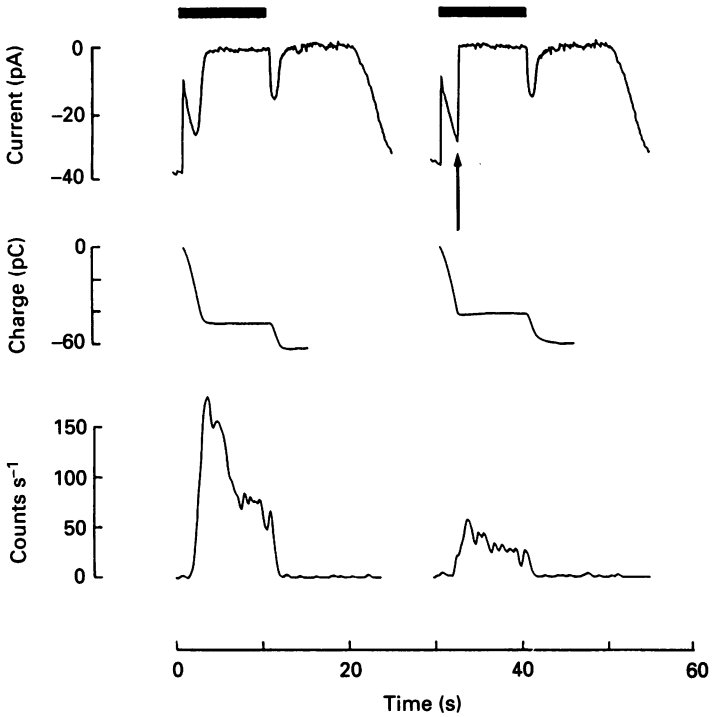

Fig. 1. Estimation of the fraction of aequorin in the outer segment, and of the rate of equilibration of aequorin between the inner and outer segments. $[Ca^{2+}]_i$ in the outer segment was repeatedly elevated by exposure to a solution of isotonic $CaCl_2$ with 500 μM-IBMX (duration of exposure shown by filled bars). The first two traces from the series are shown; time scale is continuous. The influx of Ca^{2+} was terminated in the first trace by the aequorin light emission and in subsequent traces by bright flashes (arrow in second trace). Top, outer segment membrane current (corrected for junction current; see Hodgkin *et al.* 1987). The transient current observed on restoration of normal $[Na^+]_o$ is the electrogenic Na^+–Ca^{2+}, K^+ exchange current. Middle, integral of currents in top traces. Zero levels for integrals were the current in bright steady light. Bottom, aequorin light signals. Time constant τ of decay of the aequorin light emission (see eqn (2)) at constant $[Ca^{2+}]_i$ was calculated directly from the traces (for first trace $\tau = 5{\cdot}8$ s, from which we obtain $f = 0{\cdot}22$; see eqn (3)). Time constant of replenishment of aequorin from the inner segment was obtained from the recovery of the aequorin signal between exposures to elevated $[Ca^{2+}]_i$ (mean value $128 \pm 1{\cdot}5$ s; three determinations; see Methods). There appears to be no recovery of signal in the second trace shown here, but from the integral of calcium influx it can be seen that less calcium entered on the second exposure; when this was allowed for some recovery was observed in this and all other experiments.

identical, demonstrating that the process of phototransduction is not significantly perturbed by the incorporation of aequorin into the outer segment. The only consistent difference was a decline in the light-sensitive current, usually 20–40%, which developed gradually during the period of aequorin incorporation. This decline in the light-sensitive current is not thought to be an effect of

aequorin itself, as it is also observed during the whole-cell recording in its absence. Further, after the removal of the whole-cell pipette, the light-sensitive current remained at a relatively constant amplitude for periods of up to an hour.

Collection of aequorin light

The light output from the outer segment of an aequorin-loaded rod was collected by a 100 × oil immersion objective, NA 1·3, mounted on a Zeiss IM35 microscope. A rectangular aperture at an intermediate image place, of dimensions slightly greater than the size of the image of an outer segment viewed under the 100 × objective, excluded stray light and any light emission from the inner segment without affecting the collection of aequorin light from the outer segment.

Aequorin light emission was recorded with a low-noise photomultiplier tube with a 10 mm cathode (EMI type 9789, bialkali cathode), mounted in place of the binocular head. The dark count rate of the tube was measured at the end of each experiment and at the operating voltage of 1·1 kV was around 1 count s^{-1}. The dark rate was not significantly elevated by opening the shutter in the absence of a preparation, showing that the light-proofing was adequate to ensure that no stray light reached the recording system. Counts were collected by a quantum photometer (Brookdeal type 9511/5032) with a discriminator input. Counting was inhibited during the 20 ms flashes of light by simultaneously applying a 30 ms pulse to the inhibitor on the photometer.

The total number of counts recorded during a given test exposure was displayed by a gated 1 MHz counter (Malden Electronics, model 8836). The photometer output was also stored as pulses decaying with a 10 ms time constant on analog tape (Racal Store 7DS), and was later digitized (usually at 40 Hz) on a PDP 11-73 computer, after filtering at 20 Hz with a eight-pole Bessel filter (Kemo). Further digital filtering was carried out by convolution of the aequorin signal with a Gaussian filter; the S.D. of the filter is given where appropriate in the figure legends.

Calculation of free $[Ca^{2+}]_i$ *from the aequorin light output*

To calculate the free $[Ca^{2+}]$ in the outer segment cytoplasm the rate of decay of aequorin, R, must be obtained as a function of time. R is equal to the count rate c recorded by the photomultiplier, divided by the number of counts (C_{os}) which would be recorded from the outer segment if all counts were rapidly expended:

$$R = c/C_{os}. \tag{1}$$

If aequorin is free to diffuse between inner and outer segments then in the steady state C_{os} will be a constant fraction of the total number of counts in the cell, C_t. The total number of counts remaining in the cell at the end of the experiment was obtained by lysing the cell in a hypotonic solution of 1 mM-$CaCl_2$; the aperture which restricted light collection to the outer segment was removed so that the counts from the whole cell were recorded. C_t could then be calculated at any earlier time by adding the counts recorded after that time to the total counts collected on lysis. The recorded counts were only collected from the outer segment, but little aequorin signal is observed from the inner segment (Cervetto, McNaughton & Nunn, 1985) so that the error involved in ignoring inner segment counts is small. The number of counts consumed during an entire experiment was normally no more than 20% of the total counts recorded on lysis.

The fraction of total counts present in the outer segment ($f = C_{os}/C_t$) was estimated in two ways.

(i) By direct measurement of relative volumes. A sample of ten rods was measured from video recordings and the relative volumes of the inner and outer segment were calculated. Assuming that half the outer segment is occupied by discs the value of f was $0{\cdot}26 \pm 0{\cdot}04$.

(ii) From the decay of the aequorin signal at a constant high $[Ca^{2+}]_i$, caused by exposure to isotonic $CaCl_2$ solution containing 0·5 mM-IBMX (see Fig. 1). Since in these conditions calcium is not pumped from the outer segment nor sequestered in a time-dependent manner (see below) the decline in the aequorin light output can be attributed to the consumption of aequorin by the high $[Ca^{2+}]_i$. The time constant of decline, τ, is therefore equal to the reciprocal of the decay rate, R, recorded at the start of the exposure. Therefore, from eqn (1)

$$R = 1/\tau = c/fC_t, \tag{2}$$

and so

$$f = \tau c/C_t. \tag{3}$$

The value of f in the experiment shown in Fig. 1 was 0·22, which is in good agreement with the estimate of 0·26 obtained by direct measurement. As an approximation the value of f was taken to be 0·25 in all experiments.

The analysis presented above assumes that on the time scale of a few seconds the aequorin consumed in the outer segment is not replenished from the inner segment. This assumption was

checked by testing the recovery of the outer segment aequorin concentration after a substantial exhaustion, such as that shown in the first trace of Fig. 1, by further test exposures to an elevated internal $[Ca^{2+}]$ (e.g. second trace in Fig. 1). After allowing for differences in calcium influx in the various traces the peak level of light emission on reintroducing high $[Ca^{2+}]$ after a period of rest was always found to be greater than at the end of the preceding trace, as expected if the aequorin concentration in the outer segment recovers by replenishment from the inner segment. From the increase in initial emission after a rest period the time constant of replenishment can be obtained, and in the cell shown in Fig. 1 was found to be $128 \pm 1{\cdot}5$ s (mean $\pm$ S.E.M.; three trials). Most of the experiments to be described involve elevations in $[Ca^{2+}]_i$ lasting less than 10 s, and on this time scale the replenishment of aequorin from the inner segment can be ignored. When a large fraction of the aequorin in the outer segment was depleted, however, it was important to allow sufficient time (about 5 min) for aequorin to re-equilibrate between the inner and the outer segments before continuing with further exposures to test solutions.

The decay rate R (eqn (1)) was converted into free $[Ca^{2+}]_i$ as follows (see also Blinks, Wier, Hess & Prendergast, 1982). The maximum rate of decay at saturating level of Ca^{2+}, R_{max}, was determined by injecting 10 μl of dialysed aequorin solution into 5 ml of the patch pipette solution containing 200 μM-free Ca^{2+}. At 20 °C, R_{max} was found to be $1{\cdot}05 \pm 0{\cdot}04$ s^{-1} (mean $\pm$ S.E.M.). This estimate was tested in more physiological conditions by measuring R_{max} after rods had been lysed in a hypotonic solution containing 1 mM-Ca^{2+} at the end of experiments. Under these conditions, R_{max} was found to be $0{\cdot}96 \pm 0{\cdot}21$ s^{-1}, in good agreement with the *in vitro* measurement. The fractional decay rate, $r = R/R_{max}$, was then converted into free $[Ca^{2+}]$ using a calibration curve supplied by Dr J. Blinks for the particular batch of aequorin used in these experiments. The main factor likely to affect the validity of the calibration is the intracellular free $[Mg^{2+}]$, as aequorin is weakly sensitive to Mg^{2+}. The ionized $[Mg^{2+}]$ in the pipette filling solution was 1 mM, and this value was assumed in converting aequorin light to free $[Ca^{2+}]_i$. This value of 1 mM is close to the free $[Mg^{2+}]_i$ observed in other cells, but it should be borne in mind that the free $[Ca^{2+}]_i$ measurements reported here depend on this assumption. If $[Mg^{2+}]_i$ was 2 mM, for instance, the free $[Ca^{2+}]_i$ values would be about 1·6-fold larger.

With the assumption of $[Mg^{2+}]_i = 1$ mM the calibration curve over the range $0{\cdot}1\ \mu M < [Ca^{2+}] < 30\ \mu M$ is well approximated by the function

$$[Ca^{2+}] = 50{\cdot}14r^{0{\cdot}4171}, \tag{4}$$

where $[Ca^{2+}]$ is in micromolar amounts.

Effect of spatial inhomogeneities in $[Ca^{2+}]_i$

Aequorin is a small protein (mol. wt = 20000) and so presumably diffuses into the space between the outer segment discs. The rate of aequorin light emission will therefore depend upon $[Ca^{2+}]_i$ throughout the outer segment. However, the relation between $[Ca^{2+}]_i$ and the rate of aequorin light emission is non-linear, and if there are gradients in the free $[Ca^{2+}]$ within the cell the light emitted from regions of high $[Ca^{2+}]$ will dominate the signal (Baker *et al.* 1971).

The time course of relaxation of a non-uniform gradient of $[Ca^{2+}]$ across the outer segment was estimated as follows. The distribution of a diffusible substance in a cylindrical domain after a stepwise elevation in concentration at the boundary is given by eqn 7.6.11 of Carslaw & Jaeger (1959), and is characterized by a time constant $\tau = a^2/D$, where a is the radius of the cylinder and D the effective diffusion coefficient. The diffusion coefficient of a substance which is rapidly and reversibly bound varies in proportion to the ratio of free to total concentration of the substance (Crank, 1956); the binding of calcium in the outer segment is found to be rapid and reversible, and at $[Ca^{2+}]_i > 2\ \mu M$ the ratio of free to total concentration is 0·06 (see below, p. 131). Using a free-solution diffusion coefficient for Ca^{2+} of $7{\cdot}8 \times 10^{-6}$ $cm^2\ s^{-1}$ at 20 °C (Robinson & Stokes, 1959) we obtain $\tau = 486$ ms. The mean $[Ca^{2+}]_i$ rises to one-half of its steady-state value in $0{\cdot}062\tau$ (Carslaw & Jaeger, 1959), or in 30 ms. The $[Ca^{2+}]$ reported by the aequorin signal can be obtained by including the 2·3 power relationship between $[Ca^{2+}]$ and aequorin light output; the effect is to speed the response to a rise in $[Ca^{2+}]$ at the outer segment membrane, and to slow the response to a fall, with the half-times to steady state in each case being 12·9 and 47 ms respectively. These times are all much shorter than the time constant of transport of $[Ca^{2+}]_i$ from the cell (typically of the order of 700 ms) and for all practical purposes the distribution of $[Ca^{2+}]$ across the cell can therefore be assumed to be uniform, and the aequorin signal can be taken as a reliable index of the mean free $[Ca^{2+}]_i$. Similarly, the response time of aequorin (about 10 ms, Blinks *et al.* 1982) will not cause

significant distortion in the measurement of free $[Ca^{2+}]_i$ in view of the relatively slow rate of change of $[Ca^{2+}]_i$ in the present experiments.

Solutions

The filling solution for the whole-cell pipette contained (mM): potassium aspartate, 110; $MgCl_2$, 3; Na_2ATP, 1; Na_2GTP, 1; EGTA, 0·02; PIPES, 10; pH 7·2. The small amount of EGTA (or sometimes BAPTA) was added to prevent discharge of the aequorin; the contaminating [Ca] in the solution was found by atomic absorption spectrophotometry to be 6 μM, and the addition of 20 μM-EGTA was sufficient to reduce the rate of discharge of aequorin to a low level.

Ringer solution contained (mM): NaCl, 110; $CaCl_2$, 1; $MgCl_2$, 1·6; KCl, 2·5; HEPES, 10; pH 7·5. Low-Na^+ solutions were made by replacing NaCl with LiCl, and a 0 Ca^{2+} solution was made by omitting the $CaCl_2$ and adding 2 mM-EGTA or BAPTA. Isotonic Ca^{2+} solutions had the composition (mM): $CaCl_2$, 77·5; HEPES, 10. IBMX was dissolved directly to the required concentration (usually 500 μM).

The solution bathing the rod outer segment was changed by transferring the rod between two flowing streams (Hodgkin *et al.* 1985). With flow rates of 0·5–1 ml min^{-1} the solution bathing the rod was completely changed in less than 50 ms.

Symbols

Symbols used in the remainder of the text are defined as follows:

j is the magnitude of the Na^+–Ca^{2+}, K^+ exchange current.

j_{sat} is the magnitude of the Na^+–Ca^{2+}, K^+ exchange current at a saturating level of $[Ca^{2+}]_i$.

β is the fraction of the outer segment membrane current collected by the suction pipette, which was measured as the ratio of the current collected by the suction pipette to the total outer segment membrane current recorded by the whole-cell pipette at the start of the experiment. The values of β in different cells are shown in column 4 of Table 1. The mean β in thirteen experiments was $0·52 \pm 0·02$, so in cases where β was not measured reliably a value of 0·5 was assumed.

$[Ca^{2+}]_i$ is the concentration of free Ca^{2+} ions in the outer segment cytoplasm.

$[Ca^{2+}]_T$ is the total concentration of exchangeable calcium remaining to be transported from the outer segment. It should be noted that $[Ca]_T$ does not include any bound calcium which exchanges so slowly with the cytoplasmic free Ca^{2+} that it is not extruded from the cell during the time course of a typical Na^+–Ca^{2+}, K^+ exchange current (5–10 s), nor does it include the small amount of exchangeable calcium remaining in the outer segment in the presence of a bright light. Both these quantities are negligible relative to the sizes of the calcium loads used in these experiments (Lagnado & McNaughton, 1991).

K_{Ca} is the Michaelis constant for activation of the Na^+–Ca^{2+}, K^+ exchange current by free $[Ca^{2+}]_i$.

C is the capacity of the high-affinity Ca^{2+} buffer.

K_{buff} is the Michaelis constant for the binding of Ca^{2+} to the high-affinity buffer.

K_{buff} is the value of K_{buff} relative to K_{Ca}.

R is the ratio of the concentration of Ca^{2+} bound to buffers (of any type) to the free $[Ca^{2+}]_i$, so that the ratio between the *total* and free calcium concentrations is $(R+1)$. The Ca^{2+} buffering function for the outer segment is not linear, so that the value of R depends on the $[Ca^{2+}]_i$ at which it is measured.

B is the ratio of the concentration of Ca^{2+} bound to the low-affinity buffer to the free $[Ca^{2+}]_i$. The low-affinity buffer behaves linearly over the range investigated in this paper, so that B is independent of $[Ca^{2+}]_i$.

V is the outer segment cytoplasmic volume, which in salamander rods has been estimated to have an average value of 1 pl (see, for instance, Hodgkin *et al.* 1987).

Rh* is the number of rhodopsin molecules isomerized by a flash, calculated from the measured photon flux and calculated absorption cross-section of the rod.

RESULTS

The effects of light on free internal $[Ca^{2+}]$ in Ringer solution

In normal Ringer solution the free $[Ca^{2+}]$ in the rod outer segment is near the limit of resolution of the aequorin technique for three reasons: (i) the limited amount of aequorin which can be introduced into a cell as small as a rod; (ii) the relatively low

sensitivity of aequorin when the free $[Ca^{2+}]$ is below about 1 μM; and (iii) the dark noise in the photomultiplier tube used to detect the aequorin light. None the less, in two rods in which high aequorin loads were achieved, a flash bright enough to shut off the light-sensitive current was found to cause a significant fall in the free $[Ca^{2+}]$ within the outer segment.

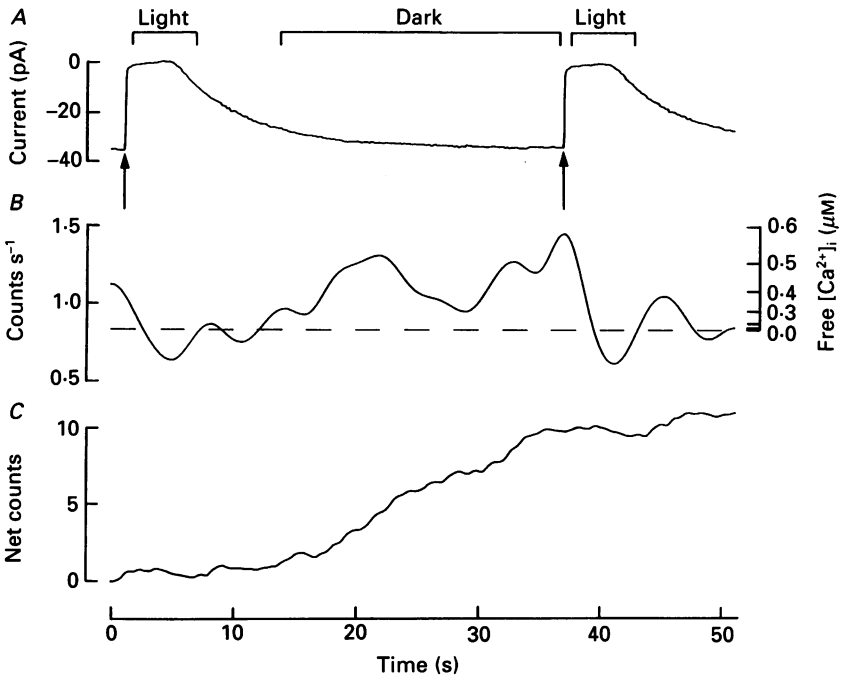

Fig. 2. Effect of light on aequorin signal in normal Ringer solution. *A*, bright flash response (flash intensity 9515 photons μm^{-2}, delivered at arrow; average of seven sweeps). *B*, aequorin light output, filtered by convolution with a Gaussian filter with standard deviation $\sigma = 1{\cdot}4$ s. Dashed trace shows background count rate of the photomultiplier tube. Net count rate (i.e. with background subtracted) has been converted to free $[Ca^{2+}]_i$ using eqn (4) (see Methods) and is shown as the right-hand ordinate; 109000 counts were recorded on lysis of this rod. The count rate over the period labelled 'light' in *A*, $0{\cdot}832 \pm 0{\cdot}137$ counts s^{-1} (mean $\pm$ S.E.M.), was not significantly different from the background count rate of $0{\cdot}909 \pm 0{\cdot}06$ counts s^{-1}, while the 'dark' rate of $1{\cdot}211 \pm 0{\cdot}064$ counts s^{-1} was highly significantly different from both ($P = 4{\cdot}4 \times 10^{-5}$ for difference between dark rate and summed light plus background). Converting the difference rate of $0{\cdot}314 \pm 0{\cdot}085$ counts s^{-1} into $[Ca^{2+}]_i$ (see Methods) gave a value of 0·41 μM. *C*, integral of trace of *B*, with background subtracted.

Figure 2*A* shows the averaged saturating flash responses from one of these cells. The filtered record of the count rate obtained from the photomultiplier tube is shown in Fig. 2*B*. The count rate in darkness was above the background rate with the shutter closed (dashed line), while after a flash the count rate was not significantly different from background. The change in the rate of aequorin light emission during the response to a flash is also illustrated by the integral of the photomultiplier tube output, from which the background rate has been subtracted (Fig. 2*C*).

The free $[Ca^{2+}]_i$ was calculated from the net count rate (i.e. after background subtraction) using eqn (4), and is shown as the right-hand ordinate in Fig. 2*B*. After a flash of light $[Ca^{2+}]_i$ declined and then recovered to the dark level of around 0·4 μM with a time course similar to that of the recovery of light-sensitive current. There was no detectable release of intracellular Ca^{2+} after the flash (upper limit of 0·2 μM).

The light-induced fall in $[Ca^{2+}]_i$ was confirmed by Student's *t* test. The count rate in a series of periods in which the light-sensitive current was at or near to its dark level ('dark' in Fig. 2*A*) was significantly above background ($P = 4{\cdot}4 \times 10^{-5}$, see Fig. 2 legend). $[Ca^{2+}]_i$ in darkness was 0·41 μM (95% confidence limits 0·30 μM $< [Ca^{2+}]_i <$ 0·49 μM), while in light $[Ca^{2+}]_i$ fell to below detectable levels ($[Ca^{2+}]_i < 0{\cdot}3$ μM at the 95% confidence level). A similar analysis on a cell loaded with 42000 recorded aequorin counts gave a value for $[Ca^{2+}]_i$ in dark of 0·42 μM, with an upper limit of 0·58 μM at the 95% confidence level.

The possibility of light-dependent Ca^{2+} release

The experiments described above show that the major effect of light is to cause a fall in $[Ca^{2+}]_i$. There have been reports of light-induced Ca^{2+} release within the outer segment of toad rods (Schröder & Fain, 1984; Fain & Schröder, 1990), and the possibility of a brief increase in $[Ca^{2+}]_i$ before the light-induced fall was therefore investigated. With the higher count rate observed in rods in which $[Ca^{2+}]_i$ had been increased by the application of IBMX (see below) measurements could be made over a shorter time window than that used in Ringer solution in Fig. 2.

The method is illustrated in Fig. 3, where the upper panel shows the light-sensitive current in a rod to which 500 μM-IBMX had been applied 3 s before the start of the trace. In trace *a* the rod was kept in darkness, but in trace *b* a bright flash lasting 20 ms was applied at 3·5 s, causing the closure of all the light-sensitive channels. The output of the photomultiplier tube during each run is shown below; the brief cessation of counting coincident with the flash in trace *b* shows where counting was inhibited during the flash. In each case the count rate was measured for a 200 ms period from 3·25 to 3·45 s (bin 1, before the flash) and for a second 200 ms period from 3·55 to 3·75 s (bin 2, after the flash).

The simplest comparison is between the count rate in bin 2 with and without a flash, but the comparison is only valid if 'dark' and 'flash' runs are interleaved to eliminate differences caused by changes in the light-sensitive current within the time required to collect a substantial number of sweeps. In one rod in which this condition was met the count rate was $47 \pm 6{\cdot}4$ counts s^{-1} in dark, and $53{\cdot}4 \pm 6{\cdot}9$ counts s^{-1} after a flash; the difference is not significant (Student's *t* test). The corresponding $[Ca^{2+}]_i$ was 7·8 μM in dark, and the release of $[Ca^{2+}]_i < 1{\cdot}0$ μM at the 95% confidence level (one-tailed *t* test).

In other rods allowance had to be made for changes in light-sensitive current in the course of a run by calculating the ratio between bin 1 and bin 2. For example, in the run illustrated in Fig. 3 the ratio bin 2/bin 1 was $1{\cdot}28 \pm 0{\cdot}17$ in dark and $1{\cdot}33 \pm 0{\cdot}12$ in runs with a flash; once again the difference is not significant. In this example $[Ca^{2+}]_i$ in dark was 9·8 μM, and increased by less than 1·1 μM after flash (95% confidence level). In six rods no detectable release of $[Ca^{2+}]_i$ was observed in the 200 ms period after a flash, with 95% confidence levels around 1 μM in well-loaded rods.

Light-sensitive channels are the major route for Ca^{2+} influx

To increase $[Ca^{2+}]_i$ to detectable levels we have in many experiments used IBMX, which increases the light-sensitive current by inhibiting the phosphodiesterase that normally hydrolyses cGMP to GMP (Cervetto & McNaughton, 1986). The traces

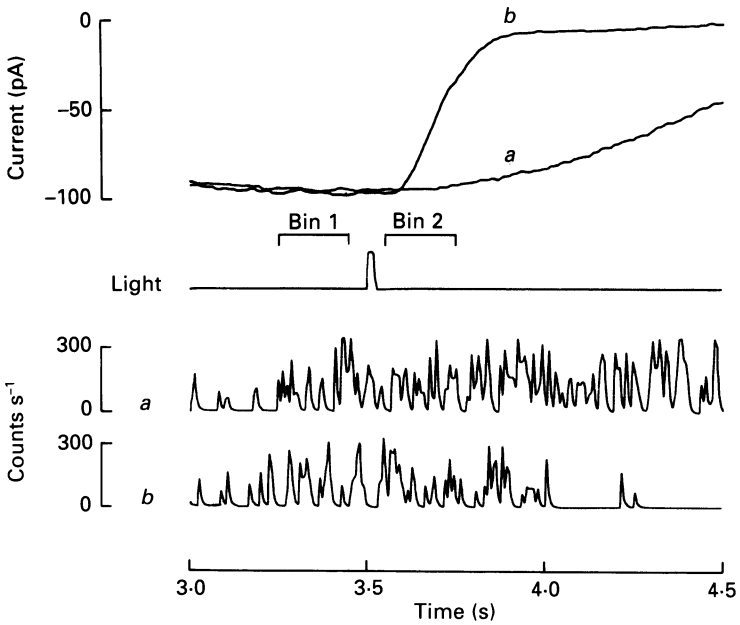

Fig. 3. Example of single traces from an experiment to examine the possibility of release of intracellular Ca^{2+} by a flash. Top traces, light-sensitive current after application of IBMX (500 μM; time scale at bottom gives time from application) in dark (*a*) and with a bright flash (*b*; flash strength 9515 photons μm^{-2}, given as shown by flash monitor under the traces). Lower traces, aequorin count rate recorded during traces *a* and *b* respectively. Note the suppression of count rate with a delay after the flash in trace *b*. Counting was inhibited for a 30 ms period coinciding with the flash in trace *b*. The periods over which counts were collected are labelled bin 1 and bin 2 (see text). Traces low-pass filtered at 80 Hz.

marked *a* in Fig. 4*A* show the response to a 7 s exposure to 500 μM-IBMX in darkness. The initial rise in light-sensitive current increased $[Ca^{2+}]_i$ and caused an increase in aequorin light emission.

The increase in $[Ca^{2+}]_i$ on exposure to IBMX could be caused by an increase in the Ca^{2+} influx, by a decrease in the efflux, or by a release of Ca^{2+} from internal stores. It is shown below (Fig. 5*C*) that IBMX has no direct effect on the activity of the Na^+–Ca^{2+}, K^+ exchange, ruling out an inhibition of Ca^{2+} efflux as the mechanism of the rise in $[Ca^{2+}]_i$. Fain & Schröder (1990) have suggested that part of the rise in $[Ca^{2+}]_i$ in response to IBMX may be due to a release of Ca^{2+} from the discs. The possibility that IBMX acts directly on the discs is tested in the experiment shown by the traces marked *b* in Fig. 4*A*, where a bright flash was delivered at the same moment as IBMX application. Suppression of the light-sensitive current was seen to

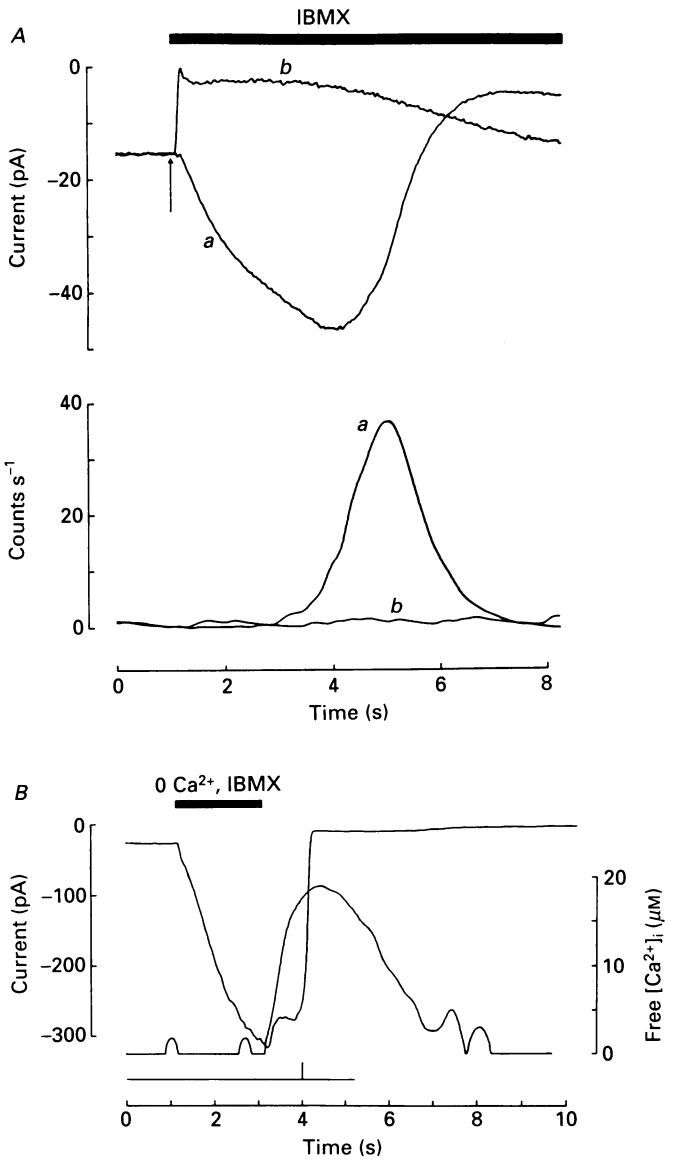

Fig. 4. *A*, effect of a bright flash on the rise in free $[Ca^{2+}]_i$ caused by IBMX (500 μM). Upper panel, outer segment membrane current recorded with a suction electrode. In trace *b* (average of two runs) a bright flash (954 photons μm^{-2}) suppressed the light-sensitive current at the moment of application of IBMX (duration of application shown by filled bar); in trace *a* (average of five runs) the exposure was carried out in darkness. Lower panel, aequorin light emission during the runs shown above. Traces smoothed by convolution with a Gaussian filter with $\sigma = 100$ ms. *B*, effect of IBMX application in the absence of external Ca^{2+}. Superimposed traces of light-sensitive current (upper trace, left-hand ordinate) and $[Ca^{2+}]_i$ (lower trace, right-hand ordinate) calculated from aequorin light output (see Methods). No significant change in $[Ca^{2+}]_i$ was observed in 0 Ca^{2+}; the large influx on readmission of 1 mM-Ca^{2+} was terminated by a bright flash (9515 photons μm^{-2}; timing shown by light monitor trace at bottom).

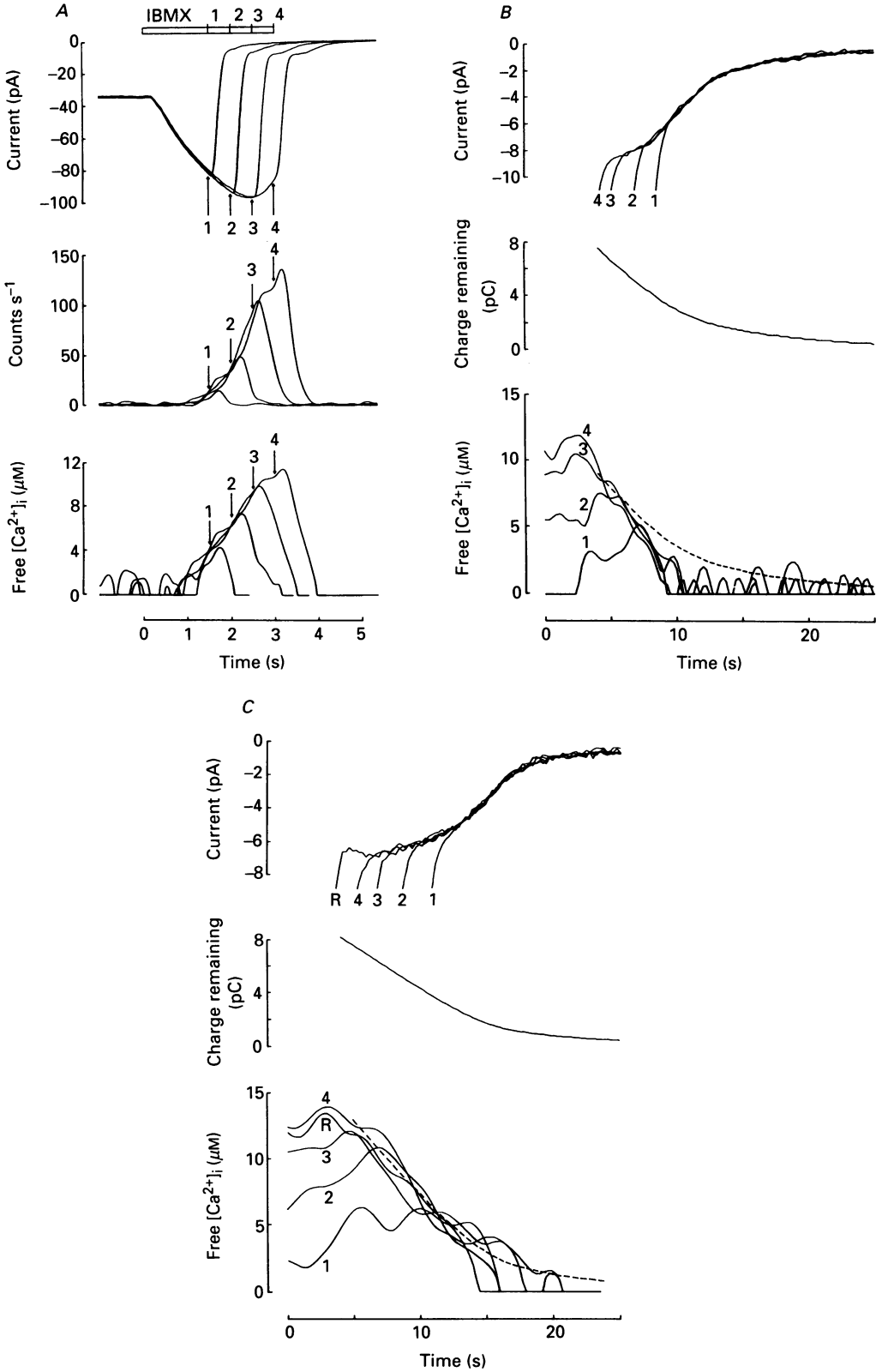

Fig. 5. For legend see facing page.

block completely the increase in free $[Ca^{2+}]_i$, ruling out the possibility of a direct action of IBMX. Alternatively, the rise in [cGMP], caused by IBMX application, might release Ca^{2+} from the discs (Puckett & Goldin, 1986). This possibility is ruled out by the experiment in Fig. 4*B*, in which the rod was exposed to IBMX in the absence of external Ca^{2+}. The large increase in light-sensitive current shows that [cGMP] had increased substantially within the outer segment, but no increase in $[Ca^{2+}]_i$ was observed. On readmission of external Ca^{2+} a large increase in $[Ca^{2+}]_i$ occurred as Ca^{2+} flowed through the increased number of open light-sensitive channels. Similar results were obtained in four rods, both in the presence and absence of IBMX.

An increase in the light-sensitive current is therefore not associated with any detectable increase in $[Ca^{2+}]_i$ unless Ca^{2+} is present in the external solution. These observations show that the principal route for entry of Ca^{2+} is through the light-sensitive channel itself. If a cGMP-dependent conductance exists in the disc membrane it can play little role in normal calcium homeostasis since when internal cGMP is raised the Ca^{2+} influx through the light-sensitive channels in the membrane far outweighs any Ca^{2+} release from an internal store.

Effect of withdrawal of external sodium on free $[Ca^{2+}]_i$

Withdrawal of external Na^+ suppresses the light-sensitive current with a delay (Yau & Nakatani, 1984*a*; Hodgkin *et al.* 1985) and, although a number of lines of evidence suggest that this suppression is due to a build-up of internal Ca^{2+} and a consequent inhibition of the guanylate cyclase (Hodgkin *et al.* 1985), a rise in $[Ca^{2+}]_i$ caused by removal of external Na^+ has not been directly demonstrated. We have

---

Fig. 5. *A*, method for measuring activation of Na^+–Ca^{2+}, K^+ exchange by $[Ca^{2+}]_i$. Top panel, light-sensitive current recorded during exposures of duration 1·5 s (1), 2·0 s (2), 2·5 s (3) and 3·0 s (4) to 0·5 mM-IBMX. A bright flash delivering $1{\cdot}9 \times 10^5$ Rh*, sufficient to suppress completely the light-sensitive current, was given as the rod outer segment was returned to Ringer solution. The increased light-sensitive current during the exposure to IBMX loads the outer segment with calcium, and the residual current observed after the saturating flash is the Na^+–Ca^{2+}, K^+ exchange current associated with the extrusion of this Ca^{2+} load. Middle panel, aequorin light output in counts s^{-1} recorded by the photomultiplier tube during the exposures shown in the top panel. Each trace is the average of four to six exposures. Signal smoothed by convolution with a Gaussian function of standard deviation $\sigma = 40$ ms. Total number of counts in the rod was 18000. Lower panel, intracellular free $[Ca^{2+}]_i$. Rod 6 of Tables 1 and 2. *B* and *C*, relation between Na^+–Ca^{2+}, K^+ exchange current (top panels), integral of exchange current (middle panels) and free $[Ca^{2+}]_i$ (lower panels), taken from two experiments of the type shown in *A*. The integral of the exchange current is also shown as a dotted trace in the lower panels. The exchange current integral is scaled arbitrarily in order to compare its time course with the time course of the decline in free $[Ca^{2+}]_i$. *B* is from the same experiment as shown in *A*. In both *B* and *C* the Na^+–Ca^{2+}, K^+ exchange currents have been brought into coincidence by translation along the time axis, and the same horizontal shift has been applied to the corresponding records of free $[Ca^{2+}]_i$. In *B* the outer segment was returned to Ringer solution as the flash was given, while in *C*, the outer segment was maintained in IBMX for traces 1–4, but in trace R was returned to Ringer solution. The similarity of the traces in *C* under the two conditions shows that the presence of IBMX has no discernible effect on the form of the Na^+–Ca^{2+}, K^+ exchange current. Part *B* from rod 6 and *C* from rod 1 of Tables 1–2.

measured the change in $[Ca^{2+}]_i$ during exposure to a Ringer solution in which Na^+ had been replaced with Li^+ by comparing count rates for a period of 10 s before and during exposure to 0 Na^+ (records not shown). In the absence of Na^+ there was a significant ($P < 5\%$) rise in $[Ca^{2+}]_i$ in both rods tested (to 2·1 and 1·7 μM).

These results demonstrate that a rise in $[Ca^{2+}]_i$ of about 2 μM is sufficient to completely inhibit the light-sensitive current, in agreement with the measurements of Koch & Stryer (1988) showing that a rise in $[Ca^{2+}]_i$ of this size is sufficient to inhibit the guanylate cyclase. The experiment also offers support for the idea that the main route for Ca^{2+} entry is through the light-sensitive channels (see preceding section), because even when calcium efflux through the Na^+–Ca^{2+}, K^+ exchange is inhibited by the withdrawal of external Na^+, the rise in $[Ca^{2+}]_i$ is small once the light-sensitive channels have been closed.

Calcium efflux through the Na^+–Ca^{2+}, K^+ exchange

The protocol used to investigate buffering and extrusion of Ca^{2+} ions is shown in Fig. 5*A*. An isolated rod with aequorin incorporated into the cytoplasm was exposed to 500 μM-IBMX in Ringer solution for periods of 1·5–3·0 s, thereby loading the outer segment with calcium. The loading period was terminated with a flash of light bright enough to close all light-sensitive channels for several seconds, and the extrusion of calcium from the outer segment by the electrogenic Na^+–Ca^{2+}, K^+ exchange was observed in the interval following the flash.

Three quantities are obtained simultaneously from the traces following the bright flash.

(i) The Na^+–Ca^{2+}, K^+ exchange current, j, is recorded directly using the suction pipette (Fig. 5*B* and *C*, upper panels). The Na^+–Ca^{2+}, K^+ exchange is the only significant membrane current following a bright flash, and the exchange is tightly coupled in a $4Na^+ : 1Ca^{2+}$, $1K^+$ stoichiometry (Cervetto *et al.* 1989) so that there is an invariant transport of one positive charge into the outer segment during the efflux of a single Ca^{2+} ion (Yau & Nakatani, 1984*b*; Hodgkin *et al.* 1987; Lagnado & McNaughton, 1991). The outer segment membrane current, when all light-sensitive channels have been closed by a bright flash, is therefore proportional to the rate of Ca^{2+} extrusion from the outer segment.

(ii) The total charge transported from the outer segment by the Na^+–Ca^{2+}, K^+ exchange is equal to the integral of the exchange current (Fig. 5*B* and *C*, centre panels). The total concentration of exchangeable calcium, $[Ca]_T$, remaining to be transported from the outer segment at time t can therefore be obtained from the following equation (symbols are defined in Methods):

$$[Ca]_T = -\frac{1}{\beta zFV}\int_t^\infty j(t')\,dt'. \tag{5}$$

(iii) The free calcium concentration within the outer segment cytoplasm, $[Ca^{2+}]_i$ (Fig. 5*A*, *B* and *C*, lower panels), is obtained from the aequorin light output.

From the three quantities j, $[Ca]_T$ and $[Ca^{2+}]_i$ the activation of the Na^+–Ca^{2+}, K^+ exchange current can be expressed as a function of $[Ca^{2+}]_i$, and the buffering of calcium in the outer segment cytoplasm can be expressed as the relation between

$[Ca]_T$ and $[Ca^{2+}]_i$. Note that the first two quantities can also be obtained from an intact rod or from an outer segment under whole-cell voltage clamp, and that some information can be obtained from this type of analysis (see below).

The duration of exposure to IBMX was varied in experiments of the type shown in Fig. 5 in order to check that the exchange current was activated by $[Ca^{2+}]_i$ in a

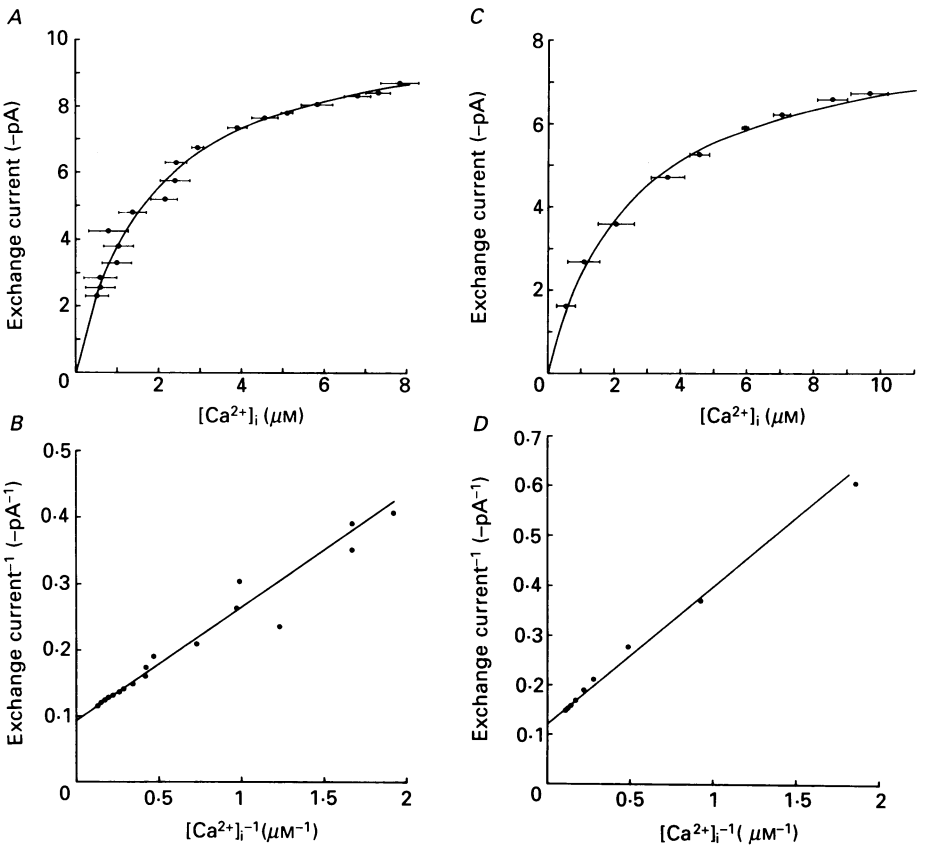

Fig. 6. Activation of the Na^+–Ca^{2+}, K^+ exchange current as a function of $[Ca^{2+}]_i$. *A* and *C*, the points plotted are taken from the top and bottom panels of Fig. 5*B* and *C*, respectively. The bars show the S.E.M. of the estimates of $[Ca^{2+}]_i$ obtained in different runs; as can be appreciated from Fig. 5, more measurements are made for each low $[Ca^{2+}]_i$ point, where the intrinsic noisiness of the signal is greater. Continuous curves are Michaelis relations with K_{Ca} = 1·8 μM and j_{sat} = 10·6 pA (*A*) and K_{Ca} = 2·3 μM and j_{sat} = 8·3 pA (*C*). *B* and *D*, Lineweaver–Burke plots of the data in *A* and *C*. Straight lines drawn with the same parameters as in *A* and *C*.

simple and reproducible manner. The single-valued relation between exchange current and free $[Ca^{2+}]_i$ is shown most clearly in Fig. 5*B* and *C*, in which the exchange currents have been brought into coincidence by shifting along the time axis. When the $[Ca^{2+}]_i$ traces are shifted by the same amount as the corresponding current traces, the falling phases of the $[Ca^{2+}]_i$ signals superimpose (lower panels in Fig. 5*B* and *C*).

Figure 5*C* also shows that IBMX has no direct effect on the Na^+–Ca^{2+}, K^+ exchange. Traces 1–4 were obtained in the presence of 500 μM-IBMX throughout, while in the trace labelled R the rod was returned to Ringer solution just as the flash was delivered. The Na^+–Ca^{2+}, K^+ exchange current in IBMX was identical in form to that observed in Ringer solution. The phosphodiesterase inhibitor is rapidly removed

TABLE 1. Activation of Na^+–Ca^{2+}, K^+ exchange current by intracellular free $[Ca^{2+}]$, determined as shown in Fig 5

(1) Cell no.	(2) K_{Ca} (μM)	(3) j_{sat} (pA)	(4) β
1	2·3	8·3	(0·5)
2	0·8	5·7	0·46
3	2·1	13.7	0·65
4	1·4	7·8	0·62
5	1·2	6·4	0·63
6	1·8	10·6	0·5
Mean ± S.E.M.	1·6 ± 0·2	8·75 ± 1·2	

Column 1 gives cell number; cell 1 is illustrated in Figs 5*C* and 6*B* and cell 6 in Figs 5*A*, 5*B* and 6*A*. Column 2 gives the Michaelis constant, K_{Ca}, for activation of Na^+–Ca^{2+}, K^+ exchange by internal free $[Ca^{2+}]$. Column 3 gives exchange current observed with a saturating internal Ca^{2+} load. Column 4 gives the ratio β of current collected by the suction pipette to the total outer segment membrane current measured by the whole-cell pipette at the start of the experiment. The mean β in thirteen experiments was 0·52 ± 0·02, so in cases where β was not measured reliably a value of 0·5 was assumed (as shown in parentheses for rod 1).

from the rod cytoplasm, as can be seen from the much more rapid rate of rise of the response compared to the response to the same flash delivered in IBMX (trace 4), and the similarity of the exchange currents in the presence and absence of IBMX cannot therefore be attributed to slow removal of the inhibitor (see also the demonstration by Hodgkin & Nunn (1988) that IBMX rapidly partitions into and out of the rod outer segment).

Activation of the Na^+–Ca^{2+}, K^+ exchange by intracellular Ca^{2+}

The relation between $[Ca^{2+}]_i$ and the Na^+–Ca^{2+}, K^+ exchange current, j, is shown for two rods in Fig. 6, obtained from the experiments shown in Fig. 5*B* and *C*. The experimental values are well fitted by the Michaelis relation:

$$\frac{j}{j_{sat}} = \frac{[Ca^{2+}]_i}{[Ca^{2+}]_i + K_{Ca}}. \quad (6)$$

The K_{Ca} differs between the two cells shown in Fig. 6, being 2·3 μM in Fig. 6*A* and *B* and 1·8 μM in Fig. 6*C* and *D*.

The mean K_{Ca} from eight determinations in six rods was 1·6 ± 0·2 μM (Table 1). In all cases the Michaelis relation provided a satisfactory fit to the experimental points, as expected if a single Ca^{2+} ion activates the exchange at the internal membrane surface. An estimate of the reliability of the determination of K_{Ca} was obtained in two rods in which K_{Ca} was determined twice, in experimental runs separated by 9·6 and 14 min, with no significant difference. The variability in the K_{Ca} obtained from

different rods (see Table 1) is therefore greater than could be explained by experimental error. A possible explanation for the variability in K_{Ca} is that the affinity may be modulated by a diffusible factor which is lost to varying degrees during the incorporation of aequorin (see below, p. 138).

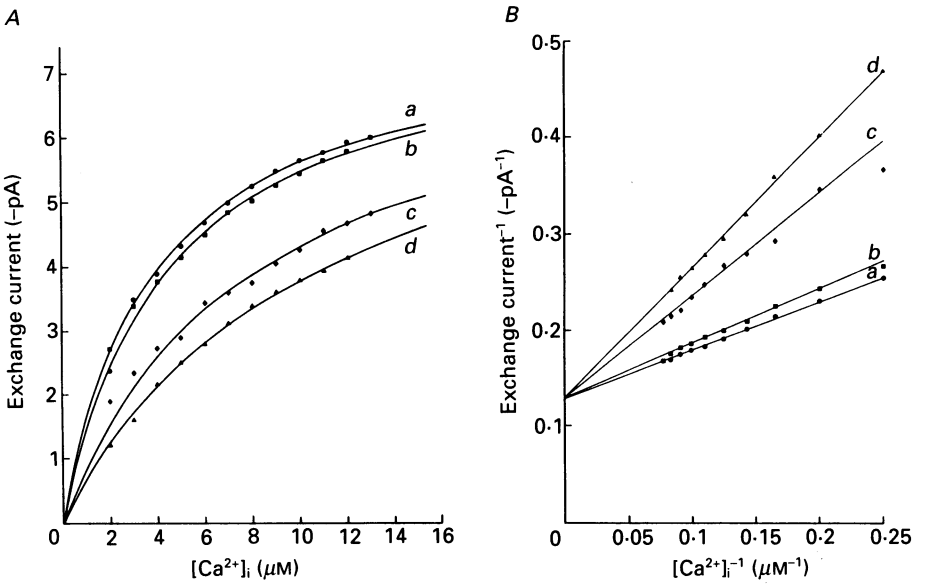

Fig. 7. *A*, dependence of Na^+–Ca^{2+}, K^+ exchange current on free $[Ca^{2+}]_i$ after various Na^+ loads. Smooth curves are drawn with values of K_{Ca} of 3·9 μM (*a*), 4·1 μM (*b*), 8·1 μM (*c*) and 10·5 μM (*d*), and all have the same value of j_{sat} = 7·8 pA. In the same rod the K_{Ca} determined as in Figs 1–3 was 1·4 μM (rod 4 of Tables 1–3). The cumulative $[Na^+]_i$ loads, assuming that the resting $[Na^+]_i$ is 10 mM and that the time constant of turnover of $[Na^+]_i$ is 100 s, were 24·2 mM (*a*), 24·6 mM (*b*), 44·4 mM (*c*) and 49·3 mM (*d*). *B*, Lineweaver–Burke plot of the data in *A*. Straight lines drawn with the same parameters.

Effect of internal $[Na^+]$ on the activation of the Na^+–Ca^{2+}, K^+ exchange by intracellular Ca^{2+}

The effects of a $[Na^+]_i$ load on the affinity of the Na^+–Ca^{2+}, K^+ exchange for intracellular Ca^{2+} are shown in Fig. 7*A* and *B*. Using the method shown in Fig. 4*B* to increase the light-sensitive current (but with IBMX omitted), a series of four Na^+ loads were introduced at intervals of 1–2 min, causing a progressive accumulation of internal Na^+. The relation between the Na^+–Ca^{2+}, K^+ exchange current and $[Ca^{2+}]_i$ as $[Na^+]_i$ increases (curves labelled *a–d* in Fig. 7) are best fitted by assuming that elevating $[Na^+]_i$ increases K_{Ca} with no effect on j_{sat} (see Lineweaver–Burke plot in Fig. 7*B*), as expected if Na^+ acts as a competitive inhibitor of the binding of Ca^{2+} at the internal membrane surface. After the first Na^+ load K_{Ca} was 3·9 μM (curve *a*), and after the fourth load it was 10·5 μM (curve *d*). The increases in $[Na^+]_i$ can be calculated by integration of the light-sensitive current during the exposure to low $[Ca^{2+}]_o$ (cf. eqn (5)), and absolute values of $[Na^+]_i$ can be roughly estimated by assuming that at rest $[Na^+]_i$ is 10 mM, and that after each Na^+ load $[Na^+]_i$ falls

towards this level along an exponential time course with a time constant of 100 s (Torre, 1982). Using these values, and taking the cytoplasmic volume of the outer segment to be 1 pl, $[Na^+]_i$ was estimated to be 24 mM after the first exposure (curve *a*, $K_{Ca} = 3{\cdot}9\ \mu M$), and 49 mM after the fourth exposure (curve *d*, $K_{Ca} = 10{\cdot}5\ \mu M$).

Time independence of the buffering of internal Ca^{2+}

In Fig. 5*B* (lower panel) the fall in free $[Ca^{2+}]_i$ is more rapid than the fall in total calcium obtained by integration ($[Ca]_T$, dashed trace in bottom panel of Fig. 5*B*). Two explanations might be advanced for this discrepancy. Equilibration of calcium between free cytoplasmic Ca^{2+} and intracellular stores could be time dependent, so that free $[Ca^{2+}]_i$ falls more rapidly than $[Ca]_T$ during extrusion of calcium. Alternatively, the buffering of $[Ca^{2+}]_i$ may be instantaneous but non-linear, with an appreciable fraction of calcium stored in a high-affinity buffer. (Note that any time dependence in the response of aequorin would impose an apparent *delay* on the fall in free $[Ca^{2+}]_i$, in the opposite direction to the observed effect.)

The two possibilities can be distinguished by comparing free $[Ca^{2+}]_i$ and $[Ca]_T$ when calcium is rising and when it is falling, because if the uptake is time dependent free $[Ca^{2+}]_i$ will lead the change in $[Ca]_T$ during both an elevation and a depletion of $[Ca^{2+}]_i$, while with an instantaneous non-linearity free $[Ca^{2+}]_i$ will lag $[Ca]_T$ during a rise and lead during a fall. Figure 8 shows an experiment to test this point. The outer segment was calcium loaded by exposure to isotonic $CaCl_2$. The Ca^{2+} influx was terminated by a bright flash and the calcium load was then extruded 8 s later by re-exposure to Ringer solution. The evidence does not favour a time-dependent uptake of calcium, for two reasons: free $[Ca^{2+}]_i$ did not lead $[Ca]_T$ during the rise in $[Ca^{2+}]_i$, and the flash halted the rise in $[Ca^{2+}]_i$ with no overshoot.

A simple model of time-dependent uptake was investigated in order to set limits on any possible time dependence of the buffering. We assume that the calcium within the cell can be either free within the cytoplasm or taken up reversibly, with time constant τ, into an intracellular store. The ratio in the steady state between bound and free $[Ca^{2+}]_i$ is B (note that we assume here a linear relation between free and bound $[Ca^{2+}]$, which is the limit at high $[Ca^{2+}]$ of eqn (8) below), and for simplicity we use the symbol Ca to mean free $[Ca^{2+}]_i$.

Then
$$\frac{d^2Ca}{dt^2} + \frac{dCa}{\tau\, dt} = -\frac{1}{\beta z F V}\left[\frac{dj}{dt} + \frac{j}{\tau(B+1)}\right]. \tag{7}$$

Equation (7) was integrated numerically using the experimentally measured calcium current and Na^+–Ca^{2+}, K^+ exchange current as the driving function j. The results shown in the lower panel of Fig. 8 are for time constants of 0 (i.e. the simple integral of calcium and exchange currents as in eqn (5)) and 30 ms. The fit using any value of time constant greater than 20 ms was appreciably worse than for $\tau = 0$ (note, for instance, the overshoot predicted to occur at the time of the flash). We conclude that the buffering of intracellular calcium is effectively instantaneous on the time scale of the light response. Results similar to those shown in Fig. 8 were seen in two further experiments.

Properties of intracellular Ca^{2+} buffers

Since the buffering of Ca^{2+} within the outer segment cytoplasm is rapid and reversible, the buffering function can be obtained by determining the relation between free $[Ca^{2+}]_i$ and $[Ca]_T$. Figure 9*A* shows this buffering curve for the rod

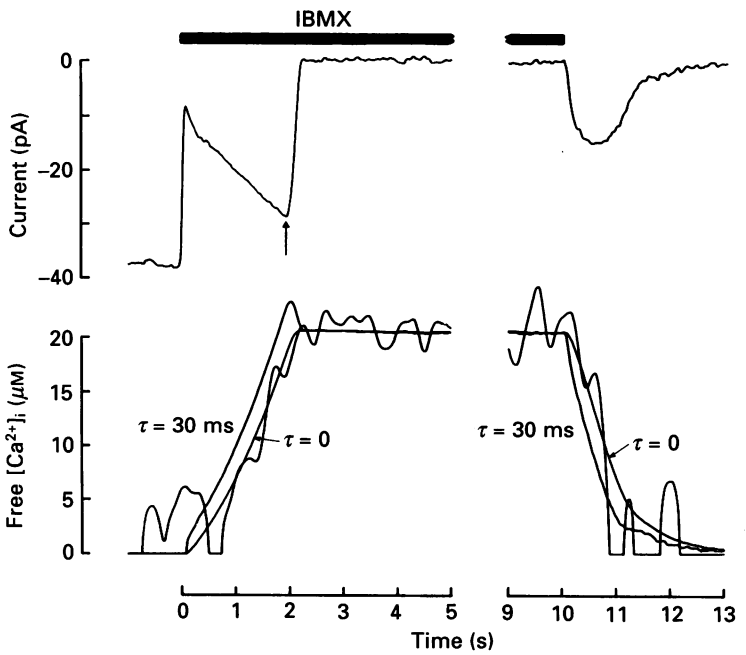

Fig. 8. Effect of a time-dependent uptake of calcium on the buffering of intracellular free $[Ca^{2+}]_i$. Top panel, membrane current recorded during exposure to isotonic $CaCl_2$, 0·5 mM-IBMX solution (duration of exposure shown by filled bar), followed by return to Ringer solution. Bright flash (4×10^4 Rh*) given at 2 s (arrow). Lower panel, intracellular free $[Ca^{2+}]_i$ (noisy trace) compared with the free $[Ca^{2+}]_i$ predicted from the total $[Ca^{2+}]_i$ by assuming that the time constant of uptake of Ca^{2+} into intracellular stores is $\tau = 0$ and 30 ms (see eqn (7)). The ratio between $[Ca^{2+}]$ bound to the buffer and free $[Ca^{2+}]_i$ was $B = 19{\cdot}8$.

illustrated in Fig. 5*C*. The buffering of Ca^{2+} was observed in all rods to have two distinct components; a high-affinity component, which was the main mechanism of calcium buffering at low $[Ca^{2+}]_i$, and a low-affinity buffer which appeared as an approximately linear relation between free $[Ca^{2+}]_i$ and $[Ca]_T$ at high $[Ca^{2+}]_i$. The capacity of the high-affinity buffer can be obtained from the intersection of the straight line through the data points at high $[Ca^{2+}]_i$ with the ordinate; in this outer segment the capacity was 35 μM. The Michaelis constant of calcium binding to the high-affinity buffer, K_{buff}, was below the limit of resolution of the aequorin signal, i.e. less than 0·7 μM. The low-affinity buffer showed no sign, in any of the rods studied using this technique, of saturation at the highest $[Ca^{2+}]_i$ which could be investigated using aequorin (approximately 20 μM).

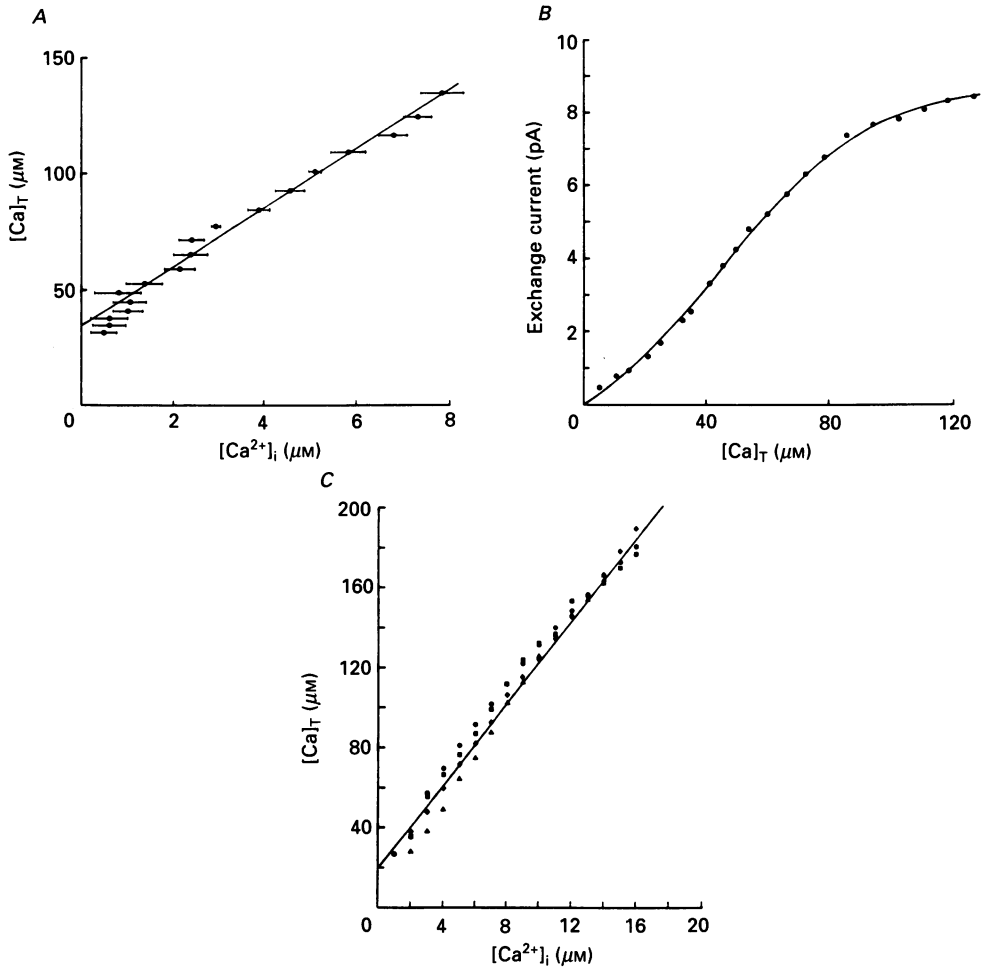

Fig. 9. Properties of intracellular calcium buffers in an aequorin-loaded outer segment. *A*, relation between $[Ca]_T$, determined from the integral of the Na^+–Ca^{2+}, K^+ exchange current, and the free $[Ca^{2+}]_i$ (data from Fig. 5*B*; rod 6 of Tables 1–3). The high-affinity buffer has a capacity of 35 μM (intercept with ordinate). The low-affinity buffering system is characterized by a line with a slope $B+1$ (see eqn (8)), where $B = 11{\cdot}7$ in this experiment. *B*, relation between Na^+–Ca^{2+}, K^+ exchange current (ordinate) and $[Ca]_T$ in the same rod. The non-Michaelis form of the relation is due to the non-linear relation between free $[Ca^{2+}]_i$ and $[Ca]_T$ as shown in *A* (see also Hodgkin *et al.* 1987). Curve drawn by eye. *C*, effect of $[Na^+]_i$ loads on the intracellular buffering of calcium. Data from the same experiment as in Fig. 7. Symbols as in Fig. 7. Straight line drawn with slope of $B+1 = 10{\cdot}3$ and intercept 20 μM.

The overall buffering power of the rod cytoplasm in the range $0 < [Ca^{2+}]_i < 20$ μM was well described in all rods by the relation:

$$[Ca]_T = \frac{C[Ca^{2+}]_i}{[Ca^{2+}]_i + K_{buff}} + (B+1)[Ca^{2+}]_i, \quad (8)$$

where C is the capacity and K_{buff} the Michaelis constant of the high-affinity buffer,

and B is the ratio of $[Ca^{2+}]_i$ bound to the low-affinity buffer to the free $[Ca^{2+}]_i$. In the six rods shown in Table 1 the capacity of the high-affinity buffer had a value of $C = 37 \pm 7$ μM (mean $\pm$ S.E.M), and the quantity B, the slope of the low-affinity buffer, had a value of $15{\cdot}9 \pm 2{\cdot}1$. At high $[Ca^{2+}]_i$ one Ca^{2+} ion remains free out of every $B+1$, or approximately seventeen, entering the outer segment. At low $[Ca^{2+}]_i$ the buffering is more powerful because of the presence of the high-affinity buffer. The ratio of bound to free $[Ca^{2+}]_i$ at low $[Ca^{2+}]_i$ cannot be determined directly from these experiments because of the low sensitivity of aequorin, but at resting $[Ca^{2+}]_i$ in darkness it can be estimated by the methods described below to be about 74.

Incorporation of aequorin into the rod outer segment cytoplasm involves a lengthy period of internal perfusion, and as small molecules equilibrate rapidly with the rod cytoplasm (see Methods) it is reasonable to suppose that the trace amount of buffer (20 μM-EGTA or BAPTA) which must be incorporated into the pipette filling solution in order to prevent premature discharge of the aequorin will diffuse into the cell and augment the endogenous high-affinity buffer. (The calcium-binding sites on aequorin are present in sub-micromolar amounts in a typical aequorin-loaded cell, and therefore the additional buffering from this source can be neglected.) The high-affinity buffering system observed in these experiments has a mean total capacity of 37 μM, of which 20 μM may be attributed to the exogenous buffer, and the capacity of the endogenous high-affinity buffer is therefore about 17 μM in aequorin-loaded rods. We show below that the endogenous buffer in the outer segments of rods which have not been internally perfused has a considerably greater capacity than 17 μM, and that a fraction of the endogenous buffer is therefore lost during the introduction of aequorin, probably by diffusion into the whole-cell pipette.

Figure 9*B* shows the relation between the two quantities that can be determined without measuring the $[Ca^{2+}]_i$: the Na^+–Ca^{2+}, K^+ exchange current and its integral, which is proportional to $[Ca]_T$. As pointed out by Hodgkin *et al.* (1987) the relation is not well described by a first-order activation function. The experiments described here show that the 'foot' on the curve is not due to an underlying non-linearity in the interaction between free $[Ca^{2+}]_i$ and the Na^+–Ca^{2+}, K^+ exchange mechanism, as might result if two or more Ca^{2+} ions were required to activate the exchange, but can instead be attributed to the presence in the outer segment of a saturable calcium buffer of high affinity as shown in Fig. 9*A*.

Effect of internal Na^+ on intracellular Ca^{2+} buffers

Figure 9*C* shows the effect of a Na^+ load on the buffering of Ca^{2+} in a rod outer segment loaded with Na^+ (data are from the experiment shown in Fig. 7). The slope of the linear part of the buffering function is unaffected by increases in $[Na^+]_i$, which is not consistent with the idea that this component of buffering is due to a Na^+–Ca^{2+}, K^+ exchange across the disc membranes.

Calcium influx, efflux and buffering under normal conditions

The Michaelis relation between $[Ca^{2+}]_i$ and the Na^+–Ca^{2+}, K^+ exchange current can be used to estimate the dark level of $[Ca^{2+}]_i$ from the initial amplitude of the Na^+–Ca^{2+}, K^+ exchange current after a bright flash. Figure 10*A* shows the response

to a bright flash of the rod illustrated in Fig. 5*A*. The decline of the Na^+–Ca^{2+}, K^+ exchange current j after the bright flash (Fig. 10*B*) is a good fit to an exponential function with a time constant of 0·69 s and an initial amplitude, extrapolated to a time at which the light-sensitive current was half-suppressed, of 1·67 pA. In the same

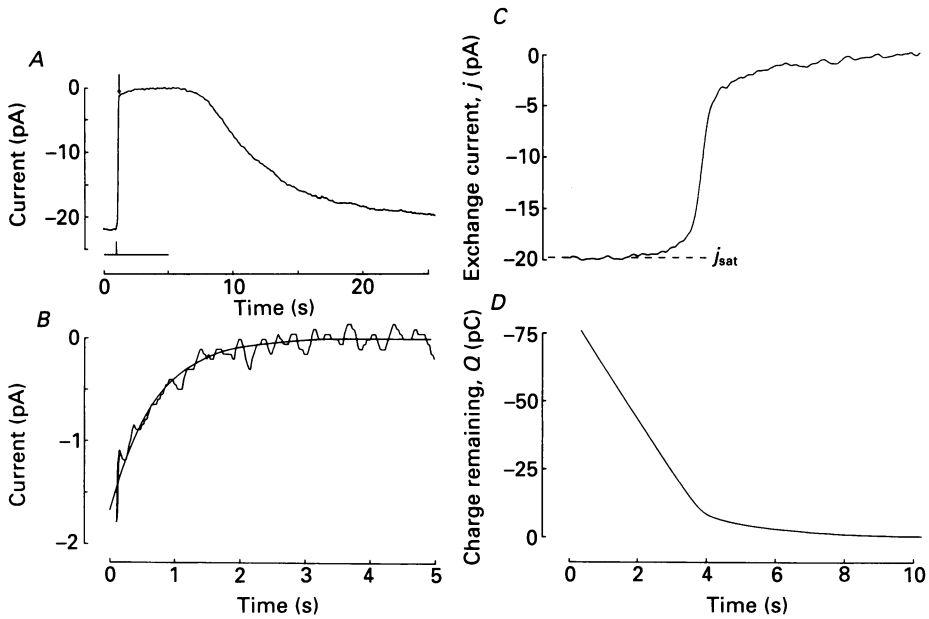

Fig. 10. *A* and *B*, calcium fluxes and buffering in an aequorin-loaded rod under normal conditions. *A*, average of six responses to a flash of intensity $1·9 \times 10^5$ Rh*. Arrow shows the Na^+–Ca^{2+}–K^+ exchange current on the plateau of the bright flash response. Dark current 21·6 pA. Rod 6 in Tables 1–3. *B*, magnified Na^+–Ca^{2+}, K^+ exchange current, taken from *A*. Time zero coincides with half-suppression of the light-sensitive current. Curve shows an exponential function with time constant 0·69 s and initial amplitude j = 1·67 pA. From this amplitude, and using the measured j_{sat} of 10·6 pA and K_{Ca} of 1·8 μM in this rod, we obtain $[Ca^{2+}]_i = 0·34$ μM. Amplitude of Na^+–Ca^{2+}, K^+ exchange current in dark, when corrected for an assumed 17 mV hyperpolarization after the bright flash using an exchange current dependence on voltage of 70 mV per e-fold change, is 1·31 pA. Calcium current in darkness is therefore 2·62 pA, or 12·1 % of the total dark current. Integral of Na^+–Ca^{2+}, K^+ exchange current is 1·15 pC, corresponding to a change in $[Ca]_T$ of 23·4 μM (eqn (5)). Ratio R between the bound and free $[Ca^{2+}]_i$ is therefore 68·9, and the Michaelis constant K_{buff} of the high-affinity buffer is 0·6 μM (see eqn (8)). *C* and *D*, method used for calculating the $[Ca^{2+}]_i$ buffering properties of an isolated, intact rod which has not been internally perfused. Rod 1 of Table 3. *C*, Na^+–Ca^{2+}, K^+ exchange current recorded in an intact rod after loading the outer segment with Ca^{2+} by exposing for 13 s to isotonic $CaCl_2$ + 0·5 mM-IBMX. The quantity $j/(j_{sat}-j)$ is calculated from this trace (see eqn (9)). *D*, integral of the exchange current, from which $[Ca]_T$ can be calculated using eqn (5).

rod the Na^+–Ca^{2+}, K^+ exchange current was found to be activated with a K_{Ca} of 1·8 μM and a j_{sat} of 10·6 pA. The $[Ca^{2+}]_i$ in darkness before the flash was obtained by rearranging eqn (6):

$$[Ca^{2+}]_i = K_{Ca}\frac{j}{j_{sat}-j}. \quad (9)$$

For this rod the change in free $[Ca^{2+}]_i$ after a flash was calculated to be 0·34 μM. Similar values obtained in the other five rods of Table 1 are presented in column 5 of Table 2. The mean change in free $[Ca^{2+}]_i$ after a flash was 0·34 μM. The exponential decline in the Na^+–Ca^{2+}, K^+ exchange current after a bright flash (Fig. 10*B*) shows that the decline in free $[Ca^{2+}]_i$ is also exponential.

TABLE 2. Characteristics of calcium influx, efflux and buffering in the outer segments of aequorin-loaded rods in Ringer solution

(1)	(2)	(3)	(4)	(5)	(6)	(7)	(8)	(9)
	J	j	τ	$[Ca^{2+}]_i$	J_{Ca}/J		K_{buff}	τ_{Ca}
Cell no.	(pA)	(pA)	(s)	(μM)	(%)	R	(μM)	(s)
1	27	1·6	0·80	0·55	9·3	52	1·07	0·71
2	18	0·8	0·61	0·13	7·1	123	0·68	0·77
3	27	2·1	0·83	0·38	12·2	67	0·84	0·66
4	23	2·2	0·80	0·54	14·7	70	0·50	0·75
5	28	0·5	0·60	0·10	2·8	61	0·30	0·72
6	23	1·7	0·69	0·34	12·1	69	0·60	0·59
Mean	24	1·5	0·72	0·34	9·7	74	0·66	0·70
± S.E.M.	± 1·6	± 0·28	± 0·04	± 0·08	± 1·7	± 10·2	± 0·11	± 0·03

Column 1 gives cell number corresponding to those in Table 1; column 2, dark current J in pA; column 3, Na^+–Ca^{2+}, K^+ exchange current j after a bright flash (not corrected for hyperpolarization); column 4, the time constant of relaxation of the Na^+–Ca^{2+}, K^+ exchange current after a bright flash; column 5, change in free $[Ca^{2+}]_i$ after a bright flash, calculated as described in the text from the magnitude of the exchange current after the flash and from the measured K_{Ca} of the Na^+–Ca^{2+}, K^+ exchange for each cell; column 6, the mean Ca^{2+} influx as a proportion of the dark current, where the Ca^{2+} influx is calculated from the magnitude of the Na^+–Ca^{2+}, K^+ exchange current after a bright flash, corrected for a 17 mV hyperpolarization (Baylor *et al.* 1984; see Cervetto *et al.* 1989); column 7, the ratio R between the bound and free $[Ca^{2+}]_i$ in Ringer solution, where the total $[Ca^{2+}]_i$ (i.e. free plus bound) is obtained from the integral of the Na^+–Ca^{2+}, K^+ exchange current (see eqn (5)) and the free $[Ca^{2+}]_i$ is from column 4; column 8, the value of K_{buff} calculated from R using the measured values of K_{Ca} and B in that rod (see eqn (11)); column 9, the calculated value of the time constant τ_{Ca} of turnover of intracellular $[Ca^{2+}]$ (see eqn (14)). See text for details.

The calcium influx in darkness can be calculated from records such as those shown in Fig. 10*A* and *B*. Since the exchange operates with a tightly coupled $4Na^+$:$1Ca^{2+}$, $1K^+$ stoichiometry (Cervetto *et al.* 1989; Lagnado & McNaughton, 1991), the current carried by Ca^{2+} is equal to twice the amplitude of the Na^+–Ca^{2+}, K^+ exchange current in the steady state in darkness. The exchange current in darkness can be estimated from initial amplitude of the exchange current after a bright flash, corrected for the hyperpolarization caused by the flash, since the flash itself does not cause any rapid change in free $[Ca^{2+}]_i$ (Figs 2 and 4). The figures in column 6 of Table 2 have been obtained on this basis, with the assumption that the steady hyperpolarization caused by the flash is 17 mV (Baylor, Matthews & Nunn, 1984) and using the voltage sensitivity of the exchange of an e-fold increase in rate per 70 mV hyperpolarization obtained by Lagnado *et al.* (1988). The mean current carried by Ca^{2+}, as a percentage of the dark current, is 9·7%, which is somewhat smaller than the figure of 15% obtained by Nakatani & Yau (1988*a*). The difference can be explained by the absence of a correction for hyperpolarization in the data of Nakatani & Yau (1988*a*); applying the correction outlined above to their measurements yields a figure of 11·7%, close to that obtained in Table 2.

The ratio of intracellular Ca^{2+} bound to rapidly exchanging buffer sites to that free in the cytoplasm can also be obtained from experiments such as that shown in Fig. 10. $[Ca]_T$ in darkness is obtained from the integral of the Na^+–Ca^{2+}, K^+ exchange current after the bright flash (eqn (1)), and the free $[Ca^{2+}]_i$ is obtained as outlined

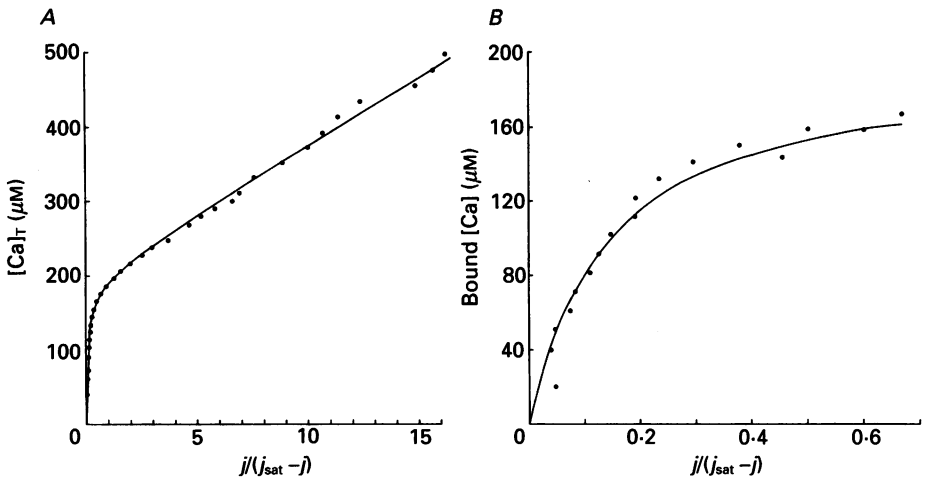

Fig. 11. *A*, intracellular $[Ca^{2+}]$ buffering properties of the intact rod shown in Fig. 10*C* and *D*. Abscissa is $j/(j_{sat}-j)$ (see eqn (9)), and the ordinate is $[Ca]_T$, the elevation of total $[Ca^{2+}]_i$ above the steady level in bright light (assuming a value for the collection ratio β of 0·5; see Methods). The form of the relation is similar to that observed in aequorin-loaded rods (cf. Fig. 9*A*) but the capacity of the high-affinity buffer, 194 μM, is almost three times greater than was observed in any of the aequorin-loaded rods. *B*, the same data as in *A* is presented on an expanded abscissa and with the linear component of buffer subtracted in order to show the Michaelis form of the high-affinity buffer. Ordinate is [bound Ca^{2+}], i.e. that fraction of $[Ca]_T$ bound to the high-affinity buffer. The curve through the points shows a Michaelis relation half-activated at $j/(j_{sat}-j) = 0{\cdot}135$. Rod 1 of Table 3.

above (see Table 2, column 5). From the ratio between the *total* and free calcium concentrations, $(R+1)$, the ratio between the *bound* and free $[Ca^{2+}]_i$, R, can be obtained, and is shown in column 7 of Table 2. The mean value of R is 74 in Ringer solution in darkness, which is considerably greater than the value of B, the ratio of $[Ca^{2+}]_i$ bound to the low-affinity buffer to the free $[Ca^{2+}]_i$ (Table 2), a difference which can be attributed to the presence in the outer segment of the saturable high-affinity buffer described above.

The Michaelis constant K_{buff} for the binding of Ca^{2+} to the high-affinity buffer can be obtained from the value of R. As $[Ca^{2+}]_i \rightarrow 0$ we obtain from eqn (8)

$$[Ca]_T/[Ca^{2+}]_i = (C/K_{buff}+B+1), \tag{10}$$

but $R+1$ is defined as

$$R+1 = [Ca]_T/[Ca^{2+}]_i,$$

and so

$$K_{buff} = C/(R-B). \tag{11}$$

Table 2, column 8, shows the values for K_{buff} obtained by this method. The mean value, 0·66 μM, is about one third of the K_{Ca} for the Na^+–Ca^{2+}, K^+– exchange determined in the same rods.

Calcium buffering in rods which have not been internally perfused

In rods which have not been loaded with aequorin the Na^+–Ca^{2+}, K^+ exchange current can be used to measure free $[Ca^{2+}]_i$ by using eqn (9). Figure 10*C* shows the

TABLE 3. Characteristics of calcium buffering in the outer segments of intact rods

(1)	(2)	(3)	(4)	(5)	(6)
	C	S	K'_{buff}	K_{buff}	K_{Ca}
Cell no.	(μM)	(μM)	(μM)	(μM)	(μM)
1	194	15·2	0·14	0·13	0·9
2	170	2·27	1·61	0·22	0·13
3	323	1·11	2·23	0·15	0·07
4	358	2·9	3·53	0·61	0·17
5	230	2·96	1·65	0·29	0·18
6	171	3·59	2·00	0·42	0·21
Mean	241	4·67	1·86	0·30	0·28
±S.E.M.	±33	±2·1	±0·45	±0·12	±0·13

Column 1 gives cell number; column 2, the capacity (C) of the high-affinity buffer, calculated as shown in Fig. 11, and assuming a collection ratio $\beta = 0{\cdot}5$ and cell volume $V = 1$ pl; column 3, the slope S of the low-affinity buffer (see Fig. 11); column 4, the ratio K'_{buff} between K_{buff} and K_{Ca} (eqn (13)); column 5, the value of K_{buff} calculated from eqns (12) and (13), assuming $B = 15{\cdot}9$; column 6, the value of K_{Ca} calculated from eqn (12) with the same assumption. Rod no. 1 is illustrated in Fig. 11.

exchange current recorded from an intact rod after a saturating load of Ca^{2+} had been introduced using a protocol similar to that shown in Fig. 8. Figure 10*D* shows the integral of the exchange current, from which $[Ca]_T$ can be obtained by the use of eqn (5). The value of $j/(j_{sat}-j)$ was calculated from the exchange current using eqn (9) and is plotted against $[Ca]_T$ in Fig. 11*A*. Similar results were obtained in six intact rods, and are summarized in Table 3. In each rod the form of the relation between $[Ca]_T$ and $[Ca^{2+}]_i$ was similar to that in aequorin-loaded outer segments; the buffering could be decomposed into a saturable high-affinity component and a low-affinity component, which confers on the buffering function a constant slope at high $[Ca^{2+}]_i$.

In Fig. 11*B* the linear part of the buffering curve in Fig. 11*A* has been subtracted to show the characteristics of the saturable Ca^{2+} buffer. The relation between the bound [Ca] and $[Ca^{2+}]_i/K_{Ca}$ can be fitted satisfactorily by a Michaelis relation.

An important difference between intact rods and those which have been internally perfused for the 10 min or so necessary to incorporate an aequorin load was the value of the capacity C of the high-affinity buffer. The capacity can be calculated as shown in Fig. 11, and its value does not depend on assuming a particular value for K_{Ca} in eqn (9). In six intact rods the mean value of C was 241 μM (column 2 in Table 3), similar to that obtained by Hodgkin *et al.* (1987), while in the six aequorin-loaded rods of Table 1 the mean value was 37 μM, a difference which was highly significant, particularly when account is taken of the 20 μM of exogenous buffer (EGTA or

BAPTA) in the aequorin-loaded rods. A probable explanation for the lower value of C in aequorin-loaded rods is that the high-affinity buffer is diffusible and is therefore partially lost in the process of internal perfusion. We show in the next section that C does indeed steadily decline during continuous internal perfusion.

From a graph such as that shown in Fig. 11*A* we can also define the slope, S, of the linear portion and the value, K'_{buff}, of $j/(j_{\text{sat}}-j)$ when the high-affinity buffer is half-saturated. Although the form of the graph is similar to that in Fig. 9*A*, the slope of the linear portion does not equal $B+1$ because the abscissa is now $[Ca^{2+}]_i/K_{Ca}$, and not $[Ca^{2+}]_i$. The relations between S and B, and between K_{buff} and K'_{buff}, are therefore:

$$B = S/K_{Ca} - 1, \tag{12}$$

and

$$K_{\text{buff}} = K'_{\text{buff}} K_{Ca}. \tag{13}$$

The quantities S and K'_{buff} are shown in columns 3 and 4 of Table 3. From eqns (12) and (13) two of the three unknowns – B, K_{Ca} and K_{buff} – can be obtained by assuming the value of the third to be the same as in aequorin-loaded rods. If K_{Ca} is assumed to have the mean value of 1·6 μM found in aequorin-loaded rods then the apparent binding ratio B of the low-affinity buffer is much less than in aequorin-loaded rods, while the value of K_{buff} is considerably larger than the rather constant values (mean 0·66 μM) found in aequorin-loaded rods.

An alternative and probably more satisfactory approach is shown in columns 5–6 of Table 3, where we assume that the low-affinity buffer is a constant feature of the outer segment, perhaps associated with the density of phosphatidylserine headgroups on the surface of the disc membranes (see Discussion), and that B therefore has the value of 15·9 found in aequorin-loaded rods. This assumption is supported by the low variability in the values of B obtained in aequorin-loaded rods (see Table 2). The mean value of K_{buff} obtained by this method is 0·3 μM (column 5 in Table 3), which is similar to the value of 0·66 μM in aequorin-loaded rods. On the other hand, the Michaelis constant for binding to the Na^+–Ca^{2+}, K^+ exchange, $K_{Ca} = 0{\cdot}3$ μM, is considerably less than the corresponding value of 1·6 μM in aequorin-loaded rods, suggesting that the affinity of the Na^+–Ca^{2+}, K^+ exchange is reduced by internal perfusion.

Changes in buffering characteristics during internal perfusion

The observation that a fraction of the high-affinity buffer was lost during the period of internal perfusion necessary to incorporate aequorin prompted us to examine the changes in buffering during a period of perfusion by a whole-cell pipette. An isolated rod outer segment was continuously held in the whole-cell configuration and was periodically subjected to an internal calcium load using the method shown in Fig. 8. The Na^+–Ca^{2+}, K^+ exchange currents recorded after 3·4, 8·2 and 19 min of internal perfusion are shown in Fig. 12*A*. The amplitude of the exchange current is virtually constant, showing that the number of exchange sites and their maximum turnover rate remained unchanged, but the form of the exchange currents altered in a characteristic way during internal perfusion. The slow final relaxation, which can be attributed to the presence in the outer segment of the saturable high-affinity buffer, became smaller in amplitude, while the rate at which the exchange current came out of saturation slowed. Similar changes in the form of the exchange currents

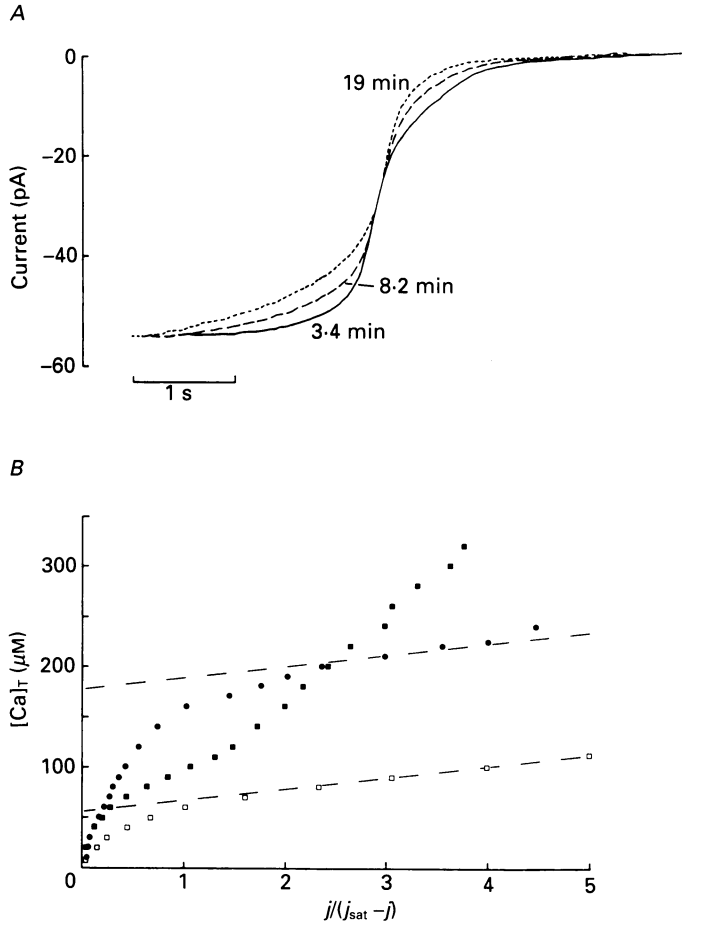

Fig. 12. *A*, effect of internal perfusion on the form of Na^+–Ca^{2+}, K^+ exchange currents. Isolated outer segment maintained under whole-cell voltage clamp (Lagnado *et al.* 1988) and loaded with Ca^{2+} by exposure to 77 mM-$CaCl_2$, 10 mM-HEPES for 6 s, with influx terminated by a bright flash after 4 s. Na^+–Ca^{2+}, K^+ exchange activated by exposure to 110 mM-Na^+, 0 Mg^{2+}, 0 Ca^{2+}, 10 mM-HEPES at $t = 6$ s. Time between commencement of internal perfusion and recording of each trace is shown alongside each trace. Pipette filling solution contained no calcium buffer, but was otherwise identical to that used in loading aequorin into rods. *B*, relation between $[Ca]_T$ (ordinate) and $j/(j_{sat}-j)$ from the traces taken at 3·4 min (●) and at 19 min (■). □ are from trace at 19 min, with horizontal axis expanded by a factor of 3·68 to produce same slope of the low-affinity buffer as at 3·4 min. Capacity C of high-affinity buffer is 177 μM at 3·4 min and 55 μM at 19 min (cf. mean value of 241 μM in intact rods; see Table 3, column 2); slope S of low-affinity buffer is 7·5 μM at 3·4 min and 27·4 μM at 19 min (cf. mean value of 4·67 μM in intact rods; see Table 3, column 3).

were seen in fifteen other outer segments which were held for a sufficiently long period of time, although the time course of onset of the changes was somewhat variable, probably because of variations in the access resistance.

The relation between $[Ca]_T$ and $j/(j_{sat}-j)$ (see eqn (9)) for the isolated outer segment of Fig. 12*A* is shown in Fig. 12*B*. The capacity C of the high-affinity buffer

declines with time, from 177 μM soon after beginning internal perfusion to 55 μM after 19 min. Figure 12*B* shows that during internal perfusion the slope S of the low-affinity buffer increases from 7·5 μM (●) to 27 μM (■), while the *relative* binding constant of the high-affinity buffer, K'_{buff}, decreases from 0·38 to 0·085. These changes could be due to parallel changes in the calcium-binding properties of the low- and high-affinity buffers, but it is difficult to see how the capacity of the low-affinity buffer could be *increased* by perfusion, as no component of the pipette filling solution is likely to increase the calcium buffering of the cell. A more plausible explanation, as outlined in the previous section, is that the affinity of the Na^+–Ca^{2+}, K^+ exchange for $[Ca^{2+}]_i$ decreases during perfusion, perhaps because the affinity of the exchange is controlled by a soluble modulator which is gradually lost with prolonged internal perfusion. Assuming that the slope B of the low-affinity buffer remains constant at 15·9 (see p. 131 and Fig. 9) we obtain from eqns (12) and (13) values for K_{Ca} of 0·44 μM after 3·4 min of perfusion and 1·6 μM, similar to the values obtained in aequorin-loaded rods, after 19 min. The K_{buff} of the high-affinity buffer remains relatively constant at 0·17 and 0·14 μM after 3·4 and 19 min of perfusion, respectively. The buffering curve after 19 min, rescaled on the assumption that the slope of the low-affinity buffer remains constant, is shown by the open squares in Fig. 12*B*, and the main change during perfusion is then a reduction in the capacity C of the high-affinity buffer, with no change in its affinity for calcium.

DISCUSSION

The free $[Ca^{2+}]_i$ in the outer segment

In two rods the free $[Ca^{2+}]_i$ in the dark was found to be close to 0·4 μM, with an upper limit of 0·5 μM at the 95% confidence level. This value is somewhat greater than, but not inconsistent with, the estimate of 0·22 μM made by Ratto *et al.* (1988) using Fura-2 in intact retinae. At these levels of internal Ca^{2+} the inhibition of the cyclase that synthesizes cGMP is likely to be substantial, since Koch & Stryer (1988) found that inhibition of the guanylate cyclase activity in bovine rods is half-maximal at a free $[Ca^{2+}]$ of around 0·1 μM. The substantial degree of inhibition of guanylate cyclase in darkness explains the large increase in light-sensitive current observed when $[Ca^{2+}]_i$ is reduced to a low level by exposing the outer segment to zero external Ca^{2+} (Hodgkin *et al.* 1984).

Using the size of the Na^+–Ca^{2+}, K^+ exchange current as an assay of the free $[Ca^{2+}]_i$ we estimate that after a bright flash $[Ca^{2+}]_i$ falls by 0·34 μM, which would bring $[Ca^{2+}]_i$ from a dark level of 0·4 μM to less than 0·1 μM. This reduction would be sufficient to cause a substantial activation of guanylate cyclase and a consequent speeding of the recovery phase of the light response. The fall in $[Ca^{2+}]_i$ may also substantially reduce the activity of the phosphodiesterase (Kawamura & Murakami, 1991).

Calcium homeostasis in the outer segment

A rise in [cGMP] within the outer segment did not cause any increase in $[Ca^{2+}]_i$ unless Ca^{2+} was present externally, showing that there is no significant cGMP-dependent release of Ca^{2+} from an intracellular store. These results, combined with

the evidence that there is no light-dependent release of internal Ca^{2+}, show that the influx of Ca^{2+} through the light-sensitive channels is the only significant entry of Ca^{2+} into the outer segment cytoplasm under normal circumstances.

The mechanism by which Ca^{2+} is removed from the outer segment also appears to be simple. After the introduction of a Ca^{2+} load, free $[Ca^{2+}]$ within the outer segment does not change unless Na^+ is present externally (see e.g. Fig. 8), showing that there is no appreciable time-dependent uptake of Ca^{2+} into an intracellular store and that the Na^+–Ca^{2+}, K^+ exchange is the major mechanism of Ca^{2+} extrusion. Although a Na^+-independent transport of Ca^{2+} by an ATP-dependent pump cannot be completely ruled out, the maximum capacity of such a system must be low in the rod outer segment, since the maximum rate of decline of free $[Ca^{2+}]_i$ in the absence of external Na^+ is less than 0·6 μM s^{-1} (McNaughton *et al.* 1986). By contrast, the Na^+–Ca^{2+}, K^+ exchange is a high-capacity transport system which can reduce the free $[Ca^{2+}]_i$ in the outer segment by rates of 30–40 μM s^{-1} when fully activated in Ringer solution.

Calcium-binding properties of the Na^+–Ca^{2+}, K^+ exchange

The ability of the Na^+–Ca^{2+}, K^+ exchange to extrude calcium far exceeds normal requirements in the rod outer segment. The saturated exchange current is an order of magnitude larger than the normal exchange current in darkness, and the mean value of 1·6 μM for the calcium binding constant, K_{Ca}, is well above the dark level of free $[Ca^{2+}]_i$.

At the outset of this study we hoped that a definite value for K_{Ca} could be obtained, so that the magnitude of the exchange current could be used as an assay of free $[Ca^{2+}]_i$ in rod outer segments without the need to incorporate a cytoplasmic calcium indicator. In fact the K_{Ca} is rather variable in different outer segments (Table 1), and there have been strong indications that affinity of the exchange for $[Ca^{2+}]_i$ may be reduced by the process of internal perfusion. The identity of the cytoplasmic modulator responsible for increasing the affinity of the exchange in intact rods is not known, but in view of the slow change in affinity during internal perfusion (p. 138) this molecule may be a soluble protein such as calmodulin or a kinase. In other cells, such as the squid giant axon, the affinity of the Na^+–Ca^{2+} exchange for external sodium and internal calcium is modulated by an ATP-dependent process (Baker & McNaughton, 1976) which depends on the presence of a calcium-dependent kinase (Dipolo & Beaugé, 1987).

Calcium buffering in the rod outer segment

The short-term buffering in the rod outer segment is rapid and reversible, and several different experiments show that two separate components are important: a high-affinity buffer, with calcium-binding constant K_{buff} of around 0·7 μM, and a low-affinity buffer which at calcium concentrations below 20 μM binds a constant proportion of the free calcium. The high-affinity buffer appears to be diffusible, because less is present in aequorin-loaded cells than in cells which have not been recorded from using a whole-cell pipette, and because its capacity declines steadily during internal perfusion of a detached outer segment (Fig. 12). The time course of the decline is not consistent with the high-affinity buffer being a small molecule,

since small molecules equilibrate between the whole-cell pipette solution and the rod interior within a minute or two (see Methods), while the high-affinity buffer is removed with a time constant of approximately 14 min (see Fig. 12). It seems likely that the high-affinity buffer is a small soluble protein which, like aequorin, is able to equilibrate slowly between the rod cytoplasm and the contents of the whole-cell pipette. The diffusion coefficient of calcium in the rod cytoplasm will be severely reduced by the presence of this high-affinity buffer; taking the capacity of the high-affinity buffer in intact rods to be 240 μM (Table 3) and its calcium binding constant to be 0·66 μM (Table 2) then 364 calcium ions will be bound for every one which is free, and the diffusion coefficient will be reduced by a factor of 365 (Crank, 1956).

The low-affinity buffer is present in a rather constant amount in aequorin-loaded rods (Table 2). This component of buffering may be associated with a fixed structure in the outer segment, such as the headgroups of the phosphatidylserine component of the disc membranes. McLaughlin & Brown (1981) have calculated that the phosphatidylserine present in rat rod outer segments will bind between six and thirty Ca^{2+} ions for every one that is free, a figure which is in good agreement with our estimate of $B = 16$. Small metabolites such as ATP and GTP may also contribute to the low-affinity component of Ca^{2+} buffering.

Time constant of changes in free $[Ca^{2+}]_i$

The time constant of turnover of intracellular free $[Ca^{2+}]$ can be related to the activity of the Na^+–Ca^{2+}, K^+ exchange, the buffering power of the cytoplasm and the outer segment volume. If the buffering is represented by eqn (8), and the Na^+–Ca^{2+}, K^+ exchange is activated in a first-order manner with binding constant K_{Ca} (eqn (6)), then it can be shown that the time constant τ_{Ca} of relaxation to the plateau after a bright flash is given by:

$$\tau_{Ca} = \frac{FV(C/K_{buff} + B + 1)}{j_{sat}/K_{Ca}}, \tag{14}$$

where j_{sat} is the absolute value (i.e. corrected for partial collection by the suction electrode; see Table 1) of exchange current at a saturating level of $[Ca^{2+}]_i$, V is the outer segment volume, F the Faraday constant and other symbols are as defined in eqn (9). For $[Ca^{2+}]_i$ near the resting level the low-affinity buffer is relatively unimportant, i.e. $B + 1 \ll C/K_{buff}$ and

$$\tau_{Ca} = FV\frac{C}{j_{sat}}\frac{K_{Ca}}{K_{buff}}. \tag{15}$$

The quantities in eqns (14) and (15) can all be measured in both intact and aequorin-loaded rods (note that although the quantities K_{Ca} and K_{buff} are not available separately in intact rods their ratio can be calculated; see eqn (13)). The values of τ predicted from eqn (14) are shown in column 9 of Table 2, and are all close to the time constant of relaxation of the Na^+–Ca^{2+}, K^+ exchange current after a bright flash in the same rods (see column 4). The mean value of 0·70 s is close to the measured mean of 0·72 s.

There are therefore a number of possible ways in which the time constant of turnover of intracellular $[Ca^{2+}]$ in a photoreceptor could be regulated. τ_{Ca} is increased

by increases in the binding constant K_{Ca} of the Na^+–Ca^{2+}, K^+ exchange, in the capacity C of the high-affinity buffer, or in the volume V of the outer segment; and it is decreased by increases in the binding constant K_{buff} of the high-affinity buffer or in the maximal Na^+–Ca^{2+}, K^+ exchange current, j_{sat}. Intact rods contain about 250 μM of a high-affinity calcium buffer (Fig. 11) which will have the effect of slowing the relaxation in intracellular free [Ca^{2+}] in response to a perturbation such as a suppression of the light-sensitive current, and therefore of slowing the onset of light adaptation which is thought to depend on the change in calcium. A possible reason for the smaller size of cones compared to rods in many species may be the need to reduce τ_{Ca}, in order to speed the process of light adaptation, by reducing the outer segment volume (Perry & McNaughton, 1991). Another interesting possibility, in view of the evidence for a regulation of the affinity of the Na^+–Ca^{2+}, K^+ exchange, is that K_{Ca} may be modulated in the process of light adaptation, thereby reducing the time constant of turnover of calcium in the light-adapted state.

This work was supported by the MRC, NATO and EEC. L.L. was a George Henry Lewes student.

REFERENCES

BAKER, P. F., HODGKIN, A. L. & RIDGEWAY, E. B. (1971). Depolarization and calcium entry in squid giant axons. *Journal of Physiology* **218**, 709–755.

BAKER, P. F. & MCNAUGHTON, P. A. (1976). Kinetics and energetics of calcium efflux from intact squid giant axons. *Journal of Physiology* **259**, 103–144.

BAYLOR, D. A., LAMB, T. D. & YAU, K.-W. (1979). The membrane current of single rod outer segments. *Journal of Physiology* **288**, 589–611.

BAYLOR, D. A., MATTHEWS, G. & NUNN, B. J. (1984). Location and function of voltage-sensitive conductances in retinal rods of the salamander, *Ambystoma tigrinum*. *Journal of Physiology* **354**, 203–224.

BLINKS, J. R., WIER, W. G., HESS, P. & PRENDERGAST, F. G. (1982). Measurement of Ca^{2+} concentrations in living cells. *Progress in Biophysics and Molecular Biology* **40**, 1–114.

BROWN, J. E., COLES, J. A. & PINTO, L. H. (1977). Effects of injections of Ca^{2+} and EGTA into the outer segment of retinal rods of *Bufo marinus*. *Journal of Physiology* **269**, 707–722.

CARSLAW, H. S. & JAEGER, J. C. (1959). *Conduction of Heat in Solids*, 2nd edn. Clarendon Press, Oxford.

CERVETTO, L., LAGNADO, L. & MCNAUGHTON, P. A. (1987). Activation of the Na:Ca exchange in salamander rods by intracellular Ca. *Journal of Physiology* **382**, 135*P*.

CERVETTO, L., LAGNADO, L. & MCNAUGHTON, P. A. (1988). The effects of internal Na on the activation of the Na: Ca exchange in isolated salamander rods. *Journal of Physiology* **407**, 81*P*.

CERVETTO, L., LAGNADO, L., PERRY, R. J., ROBINSON, D. W. & MCNAUGHTON, P. A. (1989). Extrusion of calcium from rod outer segments is driven by both sodium and potassium gradients. *Nature* **337**, 740–743.

CERVETTO, L. & MCNAUGHTON, P. A. (1986). The effects of phosphodiesterase inhibitors and lanthanum ions on the light-sensitive current of toad retinal rods. *Journal of Physiology* **370**, 91–109.

CERVETTO, L., MCNAUGHTON, P. A. & NUNN, B. J. (1985). Aequorin signals from isolated salamander rods. *Journal of Physiology* **371**, 36*P*.

CERVETTO, L., TORRE, V., RISPOLI, G. & MARRONI, P. (1985). Mechanism of light adaptation in toad rods. *Experimental Biology* **44**, 147–157.

CRANK, J. (1956). *The Mathematics of Diffusion*. Clarendon Press, Oxford.

DIPOLO, R. & BEAUGÉ, L. (1987). In squid axons, ATP modulates Na^+–Ca^{2+} exchange by a Ca_i-dependent phosphorylation. *Biochimica et Biophysica Acta* **897**, 347–354.

FAIN, G. L. & SCHRÖDER, W. H. (1985). Calcium content and calcium exchange in dark-adapted toad rods. *Journal of Physiology* **368**, 641–655.

FAIN, G. L. & SCHRÖDER, W. H. (1987). Calcium in dark-adapted toad rods: evidence for pooling and cyclic-guanosine-3′-5′-monophosphate-dependent release. *Journal of Physiology* **389**, 361–384.

FAIN, G. L. & SCHRÖDER, W. H. (1990). Light-induced calcium release and re-uptake in toad rods. *Journal of Neuroscience* **10**(7), 2238–2249.

HODGKIN, A. L., MCNAUGHTON, P. A. & NUNN, B. J. (1985). The ionic selectivity and calcium dependence of the light-sensitive pathway in toad rods. *Journal of Physiology* **358**, 447–468.

HODGKIN, A. L., MCNAUGHTON, P. A. & NUNN, B. J. (1987). Measurement of sodium–calcium exchange in salamander rods. *Journal of Physiology* **391**, 347–370.

HODGKIN, A. L., MCNAUGHTON, P. A., NUNN, B. J. & YAU, K.-W. (1984). Effects of ions on retinal rods from *Bufo marinus*. *Journal of Physiology* **350**, 649–680.

HODGKIN, A. L. & NUNN, B. J. (1988). Control of light-sensitive current in salamander rods. *Journal of Physiology* **403**, 439–471.

KAWAMURA, S. & MURAKAMI, M. (1991). Calcium-dependent regulation of cyclic GMP phosphodiesterase by a protein from frog retinal rods. *Nature* **349**, 420–423.

KOCH, K.-W. & STRYER, L. (1988). Highly cooperative feedback control of retinal rod guanylate cyclase by calcium ions. *Nature* **334**, 64–66.

LAGNADO, L., CERVETTO, L. & MCNAUGHTON, P. A. (1988). Ion transport by the Na–Ca exchange in isolated rod outer segments. *Proceedings of the National Academy of Sciences of the USA* **85**, 4548–4552.

LAGNADO, L. & MCNAUGHTON, P. A. (1991). Net charge transport during sodium-dependent calcium extrusion in isolated salamander rod outer segments. *Journal of General Physiology* **98**, 479–495.

LOLLEY, R. N. & RACZ, E. (1982). Calcium modulation of cyclic GMP synthesis in rat visual cells. *Vision Research* **22**, 1481–1486.

MCLAUGHLIN, S. & BROWN, J. E. (1981). Diffusion of Ca^{2+} ions in retinal rods. *Journal of General Physiology* **77**, 475–487.

MCNAUGHTON, P. A. (1990). The light response of vertebrate photoreceptors. *Physiological Reviews* **70**, 847–883.

MCNAUGHTON, P. A., CERVETTO, L. & NUNN, B. J. (1986). Measurement of the intracellular free calcium concentration in salamander rods. *Nature* **322**, 261–263.

MATTHEWS, H. R., MURPHY, R. L. W., FAIN, G. L. & LAMB, T. D. (1988). Photoreceptor light adaptation is mediated by cytoplasmic calcium concentration. *Nature* **334**, 67–69.

NAKATANI, K. & YAU, K.-W. (1988*a*). Calcium and magnesium fluxes across the plasma membrane of the toad rod outer segment. *Journal of Physiology* **395**, 695–729.

NAKATANI, K. & YAU, K.-W. (1988*b*). Calcium and light adaptation in retinal rods and cones. *Nature* **334**, 69–71.

PERRY, R. J. & MCNAUGHTON, P. A. (1991). Response properties of cones from the retina of the tiger salamander. *Journal of Physiology* **433**, 561–587.

PUCKETT, K. L. & GOLDIN, S. M. (1986). Guanosine 3′-5′-cyclic monophosphate stimulates release of actively accumulated calcium in purified disks from rod outer segments of bovine retina. *Biochemistry* **25**, 1739–1746.

RATTO, G. M., PAYNE, R., OWEN, W. G. & TSIEN, R. Y. (1988). The concentration of cytosolic free Ca^{2+} in vertebrate rod outer segments measured with fura 2. *Journal of Neuroscience* **8**, 3240–3246.

ROBINSON, R. A. & STOKES, R. H. (1959). *Electrolyte Solutions*, 2nd edn. Butterworth, London.

SCHRÖDER, W. H. & FAIN, G. L. (1984). Light-dependent calcium release from photoreceptors measured by laser micromass analysis. *Nature* **309**, 268–270.

TORRE, V. (1982). The contribution of the electrogenic sodium–potassium pump to the electrical activity of toad rods. *Journal of Physiology* **333**, 315–341.

YAU, K.-W. & NAKATANI, K. (1984*a*). Cation selectivity of light-sensitive conductance in retinal rods. *Nature* **309**, 352–354.

YAU, K.-W. & NAKATANI, K. (1984*b*). Electrogenic Na–Ca exchange in retinal rod outer segment. *Nature* **311**, 661–663.